Functional characterization of murine 1-acylglycerol-3-phosphate O-acyltransferase 4 (AGPAT4)

by

Ryan Bradley

A thesis
presented to the University of Waterloo
in fulfillment of the
thesis requirement for the degree of
Master of Science
in
Kinesiology

Waterloo, Ontario, Canada
© Ryan Bradley 2014

Author's Declaration

I hereby declare that I am the sole author of this thesis. This is a true copy of the thesis, including any required final revisions, as accepted by my examiners.

I understand that my thesis will be made electronically available to the public.

Ryan Bradley

Abstract

The human genome project has allowed for the rapid identification of a large number of protein families based on similarities in their genetic sequences. The acyl-glycerol phosphate acyltransferase (AGPAT) family of enzymes have been largely identified through sequence homology, with eleven isoforms identified in both mice and humans. Interestingly, very little work has been done on the characterization of AGPAT isoform 4. In the present study, I report the functional characterization of AGPAT4 as a lysophosphatidic acid acyltransferase. Although AGPAT4 is present in most tissues, I have found that it is abundant in multiple brain regions including olfactory bulbs, hippocampus, cerebellum, cortex, and brain stem, and is detectable in both primary neurons and glial cells. In assays performed *in vitro*, AGPAT4 significantly increased the incorporation of [^{14}C]oleoyl-CoA into phosphatidic acid using lysophosphatidic acid as an acyl acceptor. AGPAT4 did not display significant acyltransferase activity with lysophosphatidylcholine, lysophosphatidylethanolamine, lysophosphatidylserine, lysophosphatidylinositol, lysophosphatidylglycerol, monolysocardiolipin or dilysocardiolipin acyl acceptors. Overexpressing AGPAT4 in Sf9 cells increased the total phosphatidylinositol content, but did not significantly affect levels of other glycerophospholipids, including phosphatidic acid. Analysis of the fatty acyl profile of PA from AGPAT4-overexpressing cells indicated increased individual saturated fatty acids, particularly lauric acid (C 12:0), and arachidic acid (C 20:0). AGPAT4 localized predominately to the mitochondria, and was also regulated during embryogenesis, and in varying metabolic states. In summary, this thesis has characterized AGPAT4 as a lysophosphatidic acid acyltransferase with a potential role in mitochondrial function.

Acknowledgements

First and foremost I would like to thank my supervisor Dr. Robin Duncan, who has been of paramount importance in the development and completion of this thesis, and in shaping me in my development as a scientist. Robin, your enthusiasm and intrigue for what we do in the lab is contagious, and I have been lucky to have such a great supervisor throughout this past year and a half. You have been completely open and supportive to my ideas, and to me, your teachings will extend beyond this thesis. You have not only been a fantastic supervisor, but a wonderful life mentor as well. I look forward to what we can accomplish in the coming years. Thank you for taking a chance on me.

I would also like to thank my committee members Dr. Ken Stark and Dr. John Mielke for their insights and support throughout this project. To my lab members Phil Marvyn, Kristin Marks, Emily Mardian, Ashkan Hashemi, Marcia Domingos, and all of the undergraduates that helped in this work, thank you for all your help. Thank you to Juan J.A. Henao with his help for the *in vivo* experiments, and Steve George and Dr. Marc Aucoin for their help with the Sf9 cells. I also thank my colleagues for reminding me there is life outside the lab. To both my labmates and colleagues, your friendship and assistance throughout this thesis have been invaluable, and I wish you all the best in the future!

I would like to thank Dr. Johanna Rommens and her laboratory at the Hospital for Sick Children. Johanna, thank you for giving me my start in the lab. Rikesh, Marina, Holly, Rosa, Fan, Rashmi, Meera, and Andrew, thank you for taking time out of your days to teach me what you know. Your teachings were invaluable, and I wouldn't be where I am today without all of your help. Thank you so much.

I also could not have accomplished this thesis without the constant love and support of my parents and family, and my partner Marie-France. Mom, Dad, thank you for your reassurance and unwavering support since day one. Your endless love and guidance saw me through volunteering in a lab for an entire year, discouraged and doubting myself through to the completion of my Masters' work. Thanks for always being there, I love you both. To my sister Meghan, I could not be more proud of you. You impress me every day with your insight, caring nature, and humor. Keep working hard, you've got this! Thank you Nana for being proud of me, and for your love and support. Marie-France, thank you for keeping me sane when I doubt myself, you have been my rock. Your patience and love have kept me on course throughout some of my toughest times. I'm looking forward to what the future holds for us.

Dedication

I would like to dedicate this thesis to the memory of my grandfather, Monty Bradley.

Table of Contents

List of Tables

List of Figures

List of Abbreviations

AA: arachidonic acid
AGPAT: acylglycerol-phosphate acyltransferase
ALCAT: acyl-CoA:lysocardiolipin acyltransferase
ATP: adenosine triphosphate
BTHS: Barth Syndrome
CDP-DAG: cytidine diphosphate - diacylglycerol
CHO-K1: chinese hamster ovary-K1 cells
CL: cardiolipin
cPLA2: cytosolic A2 phospholipases
DAG: diacylglycerol
DAPI: 4'-6-diamidino-2-phenylindole
DHA: docosahexanoic acid
DLCL: dilysocardiolipin
DMEM: Dulbecco's modified eagle's medium
ETC: electron transport chain
FBS: fetal bovine serum
G3P: glycerol-3-phosphate
GC: gas chromatography
GFAP: glial fibrillary acidic protein
GFP: green fluorescent protein
GPAT: glycerol-3-phosphate acyltransferase
HA: hemagglutinin
HBSS: Hank's buffered saline solution
HEK-293: human embryonic kidney cells
IFU: infectious units
IMM: inner mitochondrial membrane
iPLA2: Ca2+ - independent A2 phospholipases
Lp-PLA2: lipoprotein-associated A2 phospholipases
LPA: lysophosphatidic acid
LPAAT: lysophosphatidic acid acyltransferase
LPC: lysophosphatidylcholine
LPE: lysophosphatidylethanolamine
LPEAT: lysophosphatidylethanolamine acyltransferase
LPG: lysophosphatidylglycerol
LPI: lysophosphatidylinositol
LPS: lysophosphatidylserine
MLCL-AT: monolysocardiolipin-acyltransferase
MLCL: monolysocardiolipin
MOI: multiplicity of infection
mtGPAT: mitochondrial glycerol-3-phosphate acyltransferase
NEM: N-ethylmaleimide
OMM: outer mitochondrial membrane
PA: phosphatidic acid
PC: phosphatidylcholine

PE: phosphatidylethanolamine
PG: phosphatidylglycerol
PGP: phosphatidylglycerol phosphate
PGPS: phosphatidylglycerol phosphate synthase
PI: phosphatidylinositol
PLA2: A2 phospholipases
PS: phosphatidylserine
PUFA: polyunsaturated fatty acid
RT-qPCR: reverse transcriptase-real time polymerase chain reaction
siRNA: small interfering RNA
sPLA2: secreted A2 phospholipases
TAG: triacylglycerol
TLC: thin layer chromatography
WAT: white adipose tissue
αTFP: α trifunctional protein

Chapter One – Introduction

Life is critically dependent on the existence of biological membranes. Present in every cell, membranes perform a variety of roles crucial to maintaining a healthy state. The plasma membrane is composed of lipids, proteins, and carbohydrates, each with a crucial role in membrane function. Phospholipids are a major lipid class found in membranes, which form the principle component of the lipid bilayer. Phospholipids are amphipathic molecules, containing both polar (phosphate heads) and non-polar (fatty acyl tails) regions. Phospholipids that contain a glycerol backbone with fatty acyl chains attached are known as glycerophospholipids. Typically, glycerophospholipids are esterified with a saturated fatty acid at the sn-1 position, and an unsaturated fatty acid at the sn-2 position (1). In addition to these hydrophobic fatty acids, a hydrophilic group is attached at the sn-3 position, which, in membranes, usually consists of a phosphate and a polar head group (2). Common examples of these polar head groups can be choline, serine, or ethanolamine, although others exist. These resultant phospholipid species are then known as phosphatidylcholine (PC), phosphatidylserine (PS), or phosphatidylethanolamine (PE), respectively.

Specific membranes will have varying compositions of glycerophospholipid species from one another, and organellar membranes can differ greatly. The outer mitochondrial membrane (OMM) is primarily composed of PC, PE, and phosphatidylinositol (PI) (3). The inner mitochondrial membrane (IMM), however, is predominated by the glycerophospholipid cardiolipin (CL), which is not present in substantial amounts on the OMM (3,4). The unique composition of these membranes is

regulated by a number of enzymes, each with their own substrate specificities. These enzymes function in the Kennedy Pathway of phospholipid and triacylglycerol *de novo* synthesis, first described by Eugene Kennedy in 1956 (5), and in Lands remodeling pathway, first described by W.E. Lands in 1958 (6). The initial composition of *de* novo synthesized phospholipids is primarily defined by the substrate specificities of glycerol-3-phosphate acyltransferases (GPATs), and acyl-glycerol phosphate acyltransferases (AGPATs), which catalyze the first two steps in *de novo* phospholipid synthesis in the classical Kennedy Pathway of glycerolipid biosynthesis. Fatty acyl chain remodeling of phospholipids by enzymes in the Land's pathway, however, can introduce substantial variation in the glycerophospholipid species that are ultimately produced.

The aim of this thesis was to characterize AGPAT isoform 4, which to date had not been fully investigated. AGPAT4 mRNA expression was analyzed by real-time reverse transcriptase polymerase chain reaction (RT-qPCR) in mouse tissues and by immunoblotting of subcellularly fractionated mouse brains. Substrate specificities of this enzyme were assessed *in vitro* through the use of radiochemical assays performed with a variety of lysophospholipid acceptors and radiolabelled oleoyl-CoA in the presence of lysates from Sf9 cells infected with baculoviral *Agpat4.* AGPAT4 activity *in vivo* was determined by assessing the fatty acid content of phospholipid fractions from Sf9 cells overexpressing AGPAT4. Finally, insight into the physiological role of AGPAT4 was examined through mRNA expression during murine embryogenesis and in varying metabolic states.

Chapter Two – Biochemical Foundations

The Kennedy Pathway of Phospholipid and Triacylglycerol Synthesis and Lands' Remodeling Pathway

The Kennedy Pathway (Figure 1) begins with the acylation of glycerol-3-phosphate (G3P) at the sn-1 position by a member of the GPAT family of proteins, forming lysophosphatidic acid (LPA). Mitochondrial GPATs (mtGPATs) prefer to esterify saturated fatty acids (7,8). Microsomal GPATs also tend to prefer saturated fatty acids although they have shown activity with unsaturated fatty acids as well (7-10). LPA is then acylated at the sn-2 position by an AGPAT to form phosphatidic acid (PA). AGPATs vary in their substrate preferences (11). A summary of AGPAT motifs in both humans and mice is seen in Table 1. Additionally, the amino acid sequence of AGPAT4 for both mice and humans is seen in Figure 2. Human and mouse amino acid sequences for AGPAT4 are identical in length and 87.8% similar, with 47 mismatched amino acids out of 365 total amino acids. Glycerophospholipid fatty acyl specificity begins with the formation of PA, but this molecule is a branching point in the Kennedy Pathway. Mitochondrial PA can either be used to form mitochondria-associated glycerophospholipids, where it is thought to move from the OMM to the IMM for the synthesis of PI, PG, or CL (12) or it can be converted into 1,2 – diacylglycerol (DAG), that is a substrate for the formation of triacylglycerol (TAG), or other polar glycerophospholipids including PC, PE, and PS.

If PA is shunted into the biosynthesis of mitochondria-specific glycerophospholipids, it is first dephosphorylated to produce DAG, which is then conjugated with cytidine diphosphate to produce cytidine diphosphate-diacylglycerol (CDP-DAG). CDP-DAG is then converted into phosphatidylglycerol phosphate (PGP) via

the enzyme phosphatidylglycerol phosphate synthase (PGPS), in the first committed step of CL biosynthesis (13). Immature CL is formed through the condensation of CDP-DAG and PG. It is then subject to remodeling in the Lands pathway (6), just as all glycerophospholipids are, through the joint action of a variety of phospholipases A_2 (PLA_2) and either acyltransferases or transacylases. There are over a dozen different known mammalian PLA_2, and they vary widely in substrate specificity, with different preferences for glycerophospholipid species and fatty acyl side chain moiety (14-17). There are also over a dozen known acyl-CoA-dependent and –independent mammalian phospholipid O-acyltransferases, and these tend to show significant acyl donor substrate specificity (14,16), and recognize only narrow classes of glycerophospholipid acyl acceptor substrates.

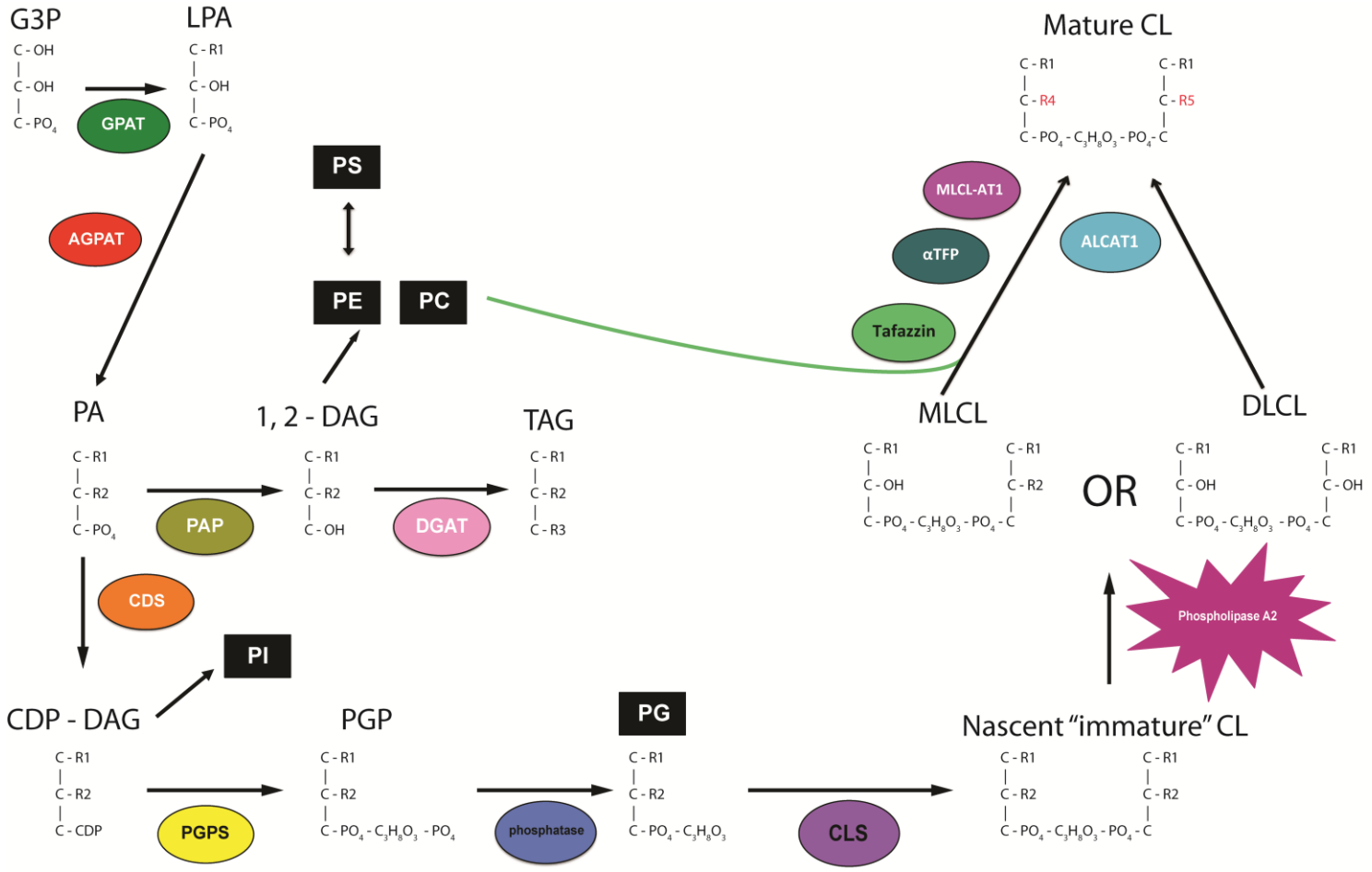

Figure 1: The Kennedy Pathway of triacylglycerol and glycerophospholipid synthesis.

Glycerol-3-phosphate acyltransferases (GPATs)

The addition of a fatty acyl-CoA to G3P converting it to LPA is the initial step performed in the Kennedy Pathway. The enzyme family responsible for this catalytic activity is the GPAT family of proteins. To date, four genes encoding for GPAT enzymes have been identified, two of which are expressed in the mitochondria. The first GPAT identified, known as mitochondrial GPAT 1 (mtGPAT1) was identified and described in 1993 (7). Expressed in the OMM, mtGPAT1 preferentially esterifies saturated fatty acids, and shows specificity for use of palmitoyl-CoA(7). Just over a decade later, the second mitochondrial GPAT was identified from rat liver mitochondria, and it was named mtGPAT2 (8). Similarly to mtGPAT1, mtGPAT2 is also expressed in the OMM. Unlike mtGPAT1 however, mtGPAT2 utilizes both saturated and unsaturated fatty acids equally well (8). The first microsomal GPAT, known now as GPAT3 was identified in 2006 (10). The second microsomal GPAT was reported in 2008 (9). Both isoforms of the microsomal GPATs show some preferential activity with saturated fatty acids, although activity has been reported with unsaturated fatty acids as well (9,10).

1-Acylglycerol-3-phosphate-O-acyltransferases (AGPATs)

The second committed step of the Kennedy Pathway is the esterification of a fatty acyl-CoA onto the sn-2 position of LPA by a member of the AGPAT family of proteins that produce PA, a branching point for either TAG or glycerophospholipid synthesis. To date, eleven isoforms of AGPATs have been identified in both mice and humans (18-26). However, detailed analysis has determined that only a few of these function primarily as classical AGPATs utilizing LPA as a major acyl acceptor, while the majority primarily exhibit remodeling activity with alternate lysophospholipid species, or else have GPAT

activity. This has lead to renaming of many of the AGPAT family members. For example, AGPAT6 has been renamed lysophosphatidylethanolamine acyltransferase (LPEAT) 2 after it was found to primarily utilize lysophosphatidylethanolamine (LPE) as an acyl acceptor (18). Likewise, AGPAT8 has been renamed acyl-CoA:lysocardiolipin acyltransferase (ALCAT) 1 since it utilizes MLCL and DLCL as acyl acceptors (27). A summary of all AGPAT isoform characterizations can be found in Table 2.

AGPAT1 was the first isoform of the AGPAT family cloned and characterized in mice (28). Biochemical specificity of AGPAT1, and later the second isoform identified, AGPAT2, were determined through microsomal substrate analysis reporting that both isoforms preferentially select oleoyl-CoA (C18:1n-9) as an acyl donor and LPA as the major acyl acceptor. In addition, AGPAT1 is also adept in employing odd-chain fatty acids (C15:0-CoA) as an acyl donor (29). Both AGPAT1 and AGPAT2 have been shown to localize to the endoplasmic reticulum (28-30). Therefore, both isoforms are thought to have similar physiological functions due to their identical substrate specificities and subcellular localization (28). AGPAT1 was shown to have highest expression in testis, with some expression in pancreas and adipose tissue, but is expressed in a broad range of tissues (19), whereas AGPAT2 was predominately expressed in adipose tissue, with some expression in liver and pancreas (29).

Both AGPAT3 and APGAT5 have been reported to localize to the endoplasmic reticulum, as well as the nuclear envelope, while AGPAT5 also localized to the mitochondria (25). AGPAT3 preferentially esterifies LPA in the presence of arachidonic acid (C20:4n-6), but will also use LPE in the presence of oleoyl-CoA (25,31). AGPAT3

has been shown to have high expression within testis (31), pancreas, and kidney (25). AGPAT5 tissue expression has been found to be high in skeletal muscle and heart, with low expression in the prostate and testis (25).

AGPAT6 and AGPAT7 have also been shown to localize to the endoplasmic reticulum (20,21). AGPAT6 preferentially uses saturated fatty acyl-CoAs including C12:0-CoA, C16:0-CoA, and C18:0-CoA (20), but does not show a preference for a lysophospholipid acceptor whereas AGPAT7 prefers longer-chain fatty acids including C16:0-CoA, C18:0-CoA, C18:1n-9-CoA (18). Oleoyl-CoA is the preferred acyl donor of AGPAT7, and LPE is the preferred acyl acceptor (18). AGPAT6 has been reported to have broad distribution within tissues, and is important in overall AGPAT activity (20). AGPAT7 showed predominant expression within brain, and is thought to have a role in phospholipid remodeling of PE (20).

AGPAT8 is predominately expressed in heart and localizes to the endoplasmic reticulum. It utilizes palmitoyl-CoA to esterify into LPA over both oleoyl-CoA, and stearoyl-CoA (22). AGPAT8 has also been shown to utilize both MLCL and DLCL to produce CL, which is its primary function *in vivo* (27). AGPAT9 shows predominant expression in lung and spleen, and was shown to prefer oleoyl-CoA as a fatty acyl donor, with LPA as the acyl acceptor (24). At the cellular level, AGPAT9 localizes to the endoplasmic reticulum, and has similar AGPAT enzymatic activity as AGPAT3, AGPAT5, and AGPAT8 (24).

Both AGPAT10 and AGPAT11 localize to the endoplasmic reticulum (23,26). AGPAT10 is more highly expressed in adipose tissue, followed by the testis, and kidney (26), whereas AGPAT11 is found to be predominately expressed in heart and skeletal

muscle (23). Both AGPAT10 and AGPAT11 utilize oleoyl-CoA to esterify into LPA (23,26).

Table 1: Summary of AGPAT protein family conserved motifs.

Motif Number	Motif	Mouse AGPAT4	Human AGPAT4	Encodes for	Reference
I	*N***H**X_4**D**	93 VLN**H**KFEI**D**FLCG	93 VLN**H**KFEI**D**FLCG	Catalysis	(32)
II	**F**X_2**R**	139 VEMI**F**CT**R**KW	139 TEMV**F**CS**R**KW	G3P Binding	(32)
III	**EGTR**	173 IHC**EGTR**FT	173 IHC**EGTR**FT	G3P Binding	(32)
IV	**P**	202 HHLL**P**RTKGFA	202 HHLL**P**RTKGFA	Catalysis	(32)

Table 2: Summarized results of AGPAT family member tissue and subcellular expression, substrate preferences, and enzyme classifications.

AGPAT Isoform	Tissue Expression	Subcellular Localization	Fatty acyl-CoA donor	Lysophospholipid acceptor	Other name(s)	References
1	Testis, pancreas, adipose tissue	Endoplasmic reticulum	C18:1-CoA C15:0-CoA	LPA	LPAAT-α	(28,29)
2	Adipose tissue, pancreas, liver	Endoplasmic reticulum	C18:1-CoA	LPA	LPAAT-β	(29)
3	Testis, pancreas, kidney	Endoplasmic reticulum, Nuclear envelope	C20:4-CoA	LPA, LPC/LPI/LPS	LPAAT-γ	(25,31)
4	**Brain, heart, renal WAT, present in most tissues**	**Mitochondria**	**C12:0-CoA** **C18:0-CoA** **C20:0-CoA**	***In vitro*: LPA** ***In vivo*: LPI**	**LPAAT-δ**	(19,25,33)
5	Skeletal muscle, heart	Endoplasmic reticulum, mitochondria	C18:1-CoA	LPA, LPE	LPAAT-ε	(25)
6	Liver, broad distribution	Endoplasmic reticulum	C16:0-CoA C18:1n-9-CoA C18:2n-6	No specificity	GPAT4 LPAAT-ζ	(10,20,34)
7	Brain	Endoplasmic reticulum	C18:1-CoA	LPE	LPEAT2, LPCAT4, LPAAT-η	(18,21)
8	Heart	Endoplasmic reticulum	C16:0-CoA	LPA, LPC, MLCL, DLCL	ALCAT1, LPCAT1	(22,27)
9	Lung, spleen	Endoplasmic reticulum	C18:1-CoA	LPA		(24)
10	Adipose tissue	Endoplasmic reticulum	C18:1-CoA	LPA	LPAAT-θ GPAT3	(26)
11	Heart, skeletal muscle	Endoplasmic reticulum	C18:1-CoA	LPA		(23)

Abbreviations: 1-acylglycerol-3-phosphate O-acyltransferase (AGPAT), white adipose tissue (WAT), lysophosphatidic acid (LPA), lysophosphatidylcholine (LPC), lysophosphatidylinositol (LPI), lysophosphatidylserine (LPS), monolysocardiolipin (MLCL), dilysocardiolipin (DLCL), lysophosphatidylethanolamine (LPE), lysophosphatidic acid acyltransferase (LPAAT), acyl-CoA:lysocardiolipin acyltransferase (ALCAT), glycerol-3-phopshate acyltransferase (GPAT), lysophosphatidylcholine acyltransferase (LPCAT), lysophosphatidylethanolamine acyltransferase (LPEAT).

AGPAT4

AGPAT4 has also been identified in both humans and mice, although characterization work on this enzyme has been limited until recently. Lu *et al*. (2005) reported that recombinant AGPAT4 synthesized in reticulocyte lysates had shown a low level of AGPAT activity with LPA (19). In the same study, however, murine AGPAT4 was expressed in COS-7 cells transfected with the mammalian expression vector pcDNA3.1-AGPAT4, and AGPAT activity was not consistently observed (19). Recently, the work of Eto *et al*. (2014) characterized AGPAT4 activity as an AGPAT, which preferentially esterifies docosahexanoic acid (DHA) into LPA in CHO-K1 cells *in vitro* (33). A significant limitation of this work is that it only included use of LPA as an acyl acceptor, and no other lysophospholipids were assayed, including mitochondrial-associated lysophospholipids including lysophosphatidylinositol (LPI), MLCL, and DLCL. In addition, only the microsomal fraction was utilized for activity assays, precluding analysis of the mitochondrial fraction that we have found contains the majority of AGPAT4 localization. The inconsistent AGPAT activity shown in these reports, along with a lack of literature characterizing this isoform with other acyl acceptors, was the basis of this thesis project.

```
Mm          1  MDLIGLLKSQ FLCHLVFCYV FIASGLIVNA IQLCTLVIWP INKQLFRKIN ARLCYCVSSQ  60
               MDLIGLLKSQ FLCHLVFCYV FIASGLIVNA IQL TL  WP INKQLFRKIN  RL YC SSQ
Hs          1  MDLAGLLKSQ FLCHLVFCYV FIASGLIINT IQLFTLLLWP INKQLFRKIN CRLSYCISSQ  60

                                                    Motif I
Mm         61  LVMLLEWWSG TECTIYTDPK ACPHYGKENA IVVLNHKFEI DFLCGWSLAE RLGILGNSKV  120
               LVMLLEWWSG TECTI TDP  A   YGKENA IVVLNHKFEI DFLCGWSL E R G LG SKV
Hs         61  LVMLLEWWSG TECTIFTDPR AYLKYGKENA IVVLNHKFEI DFLCGWSLSE RFGLLGGSKV  120

                                 Motif II                                Motif III
Mm        121  LAKKELAYVP IIGWMWYFVE MIFCTRKWEQ DRQTVAKSLL HLRDYPEKYL FLIHCEGTRF  180
               LAKKELAYVP IIGWMWYF E M FC RKWEQ DR TVA SL  HLRDYPEKY  FLIHCEGTRF
Hs        121  LAKKELAYVP IIGWMWYFTE MVFCSRKWEQ DRKTVATSLQ HLRDYPEKYF FLIHCEGTRF  180

                                       Motif IV
Mm        181  TEKKHQISMQ VAQAKGLPSL KHHLLPRTKG FAITVKCLRD VVPAVYDCTL NFRNNENPTL  240
               TEKKH ISMQ VA AKGLP L KHHLLPRTKG FAITVK LR  VV AVYDCTL NFRNNENPTL
Hs        181  TEKKHEISMQ VARAKGLPRL KHHLLPRTKG FAITVRSLRN VVSAVYDCTL NFRNNENPTL  240

Mm        241  LGVLNGKKYH ADCYVRRIPM EDIPEDEDKC SAWLHKLYQE KDAFQEEYYR TGVFPETPWV  300
               LGVLNGKKYH AD YVRRIP  EDIPED D C SAWLHKLYQE KDAFQEEYYR TG FPETP V
Hs        241  LGVLNGKKYH ADLYVRRIPL EDIPEDDDEC SAWLHKLYQE KDAFQEEYYR TGTFPETPMV  300

Mm        301  PPRRPWSLVN WLFWASLLLY PFFQFLVSMV SSGSSVTLAS LVLIFCMASM GVRWMIGVTE  360
               PPRRPW LVN WLFWASL LY PFFQFLVSM   SGSS TLAS   L F  AS  GVRWMIGVTE
Hs        301  PPRRPWTLVN WLFWASLVLY PFFQFLVSMI RSGSSLTLAS FILVFFVASV GVRWMIGVTE  360

Mm        361  IDKGSAYGNI DNKRKQTD 378
               IDKGSAYGN  DNK K  D 378
Hs        361  IDKGSAYGNS DSKQKLND 378
```

Figure 2: Amino acid sequence alignment of mouse (Mus musculus: GI 28704097) and human (Homo sapiens: GI 69128030) 1-acyl-glycerol-3-phosphate O-acyltransferase 4.

Sequences display 87.8% identity (46 mismatched amino acids), and identical chain lengths. Predicted substrate binding and catalytically active motifs are displayed in bold, with critical residues underlined. Predicted transmembrane helices are represented in grey italics.

TMHMM result

```
# Sequence Length: 378
# Sequence Number of predicted TMHs:  3
# Sequence Exp number of AAs in TMHs: 87.81176
# Sequence Exp number, first 60 AAs:  28.03487
# Sequence Total prob of N-in:        0.21657
# Sequence POSSIBLE N-term signal sequence
Sequence      TMHMM2.0      outside     1    19
Sequence      TMHMM2.0      TMhelix     20   42
Sequence      TMHMM2.0      inside      43   307
Sequence      TMHMM2.0      TMhelix     308  330
Sequence      TMHMM2.0      outside     331  334
Sequence      TMHMM2.0      TMhelix     335  357
Sequence      TMHMM2.0      inside      358  378
```

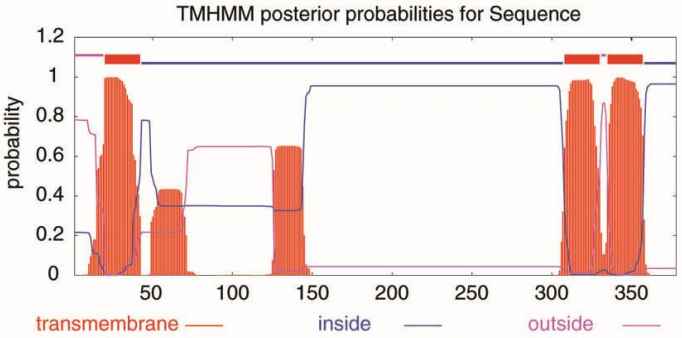

B

```
2 possible models considered, only
significant TM-segments used


the models differ in the number of TM-helices !

STRONGLY prefered model: N-terminus outside
5 strong transmembrane helices, total score:8303
 # from   to length score orientation
 1    15   39 (25)     1981 o-i
 2    53   69 (17)      915 i-o
 3   128  144 (17)      858 o-i
 4   308  326 (19)     2540 i-o
 5   329  352 (24)     2009 o-i

alternative model
4 strong transmembrane helices, total score:7411
 # from   to length score orientation
 1    13   31 (19)     2004 i-o
 2   128  144 (17)      858 o-i
 3   308  326 (19)     2540 i-o
 4   329  352 (24)     2009 o-i
```

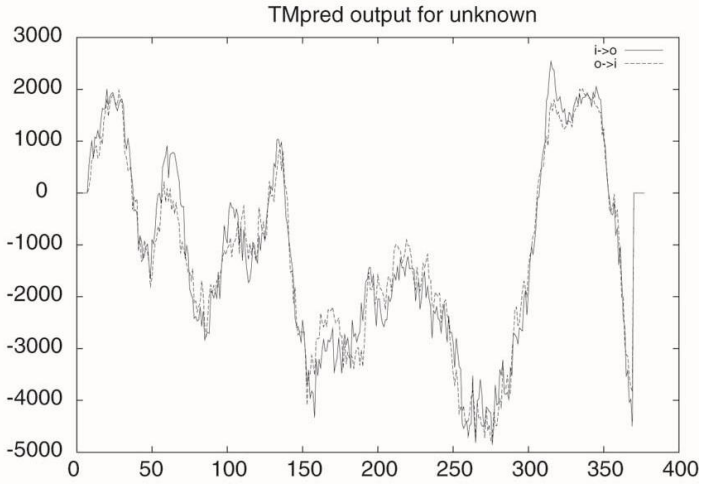

Figure 3: Kyte-Doolittle hydropathy plot of murine (Mus musculus: GI 28704097) AGPAT4 indicating from 3-5 possible transmembrane helices. *A*, a proposed K-D plot of AGPAT4). Murine 1-acyl-glycerol-phosphate O-acyltransferase 4 is 378 amino acids in length, with three strongly predicted transmembrane helices. From the N-terminus, AGPAT4 is cytosolic from the first to 19th amino acid. The 20th to 42nd amino acids span the mitochondrial membrane, while a large bulk of the protein (43rd to 307th amino acids) is inside the mitochondrial membrane. Twenty three amino acids (308-330) span the mitochondrial membrane, with a small 3 amino acid fragment becoming cytosolic once again (331-334). The protein then spans back down into the membrane from the 335th to 357th amino acids, once more entering the inner membrane space from the 358th to 378th amino acid. *B*, two other proposed K-D plots of AGPAT4. A strongly preferred model indicates 5 transmembrane helices, while an alternative model suggests 4 transmembrane helices.

Chapter Three – Rationale, Objectives, and Hypotheses

Rationale

AGPAT4 had not been fully characterized. Although two studies have been published on this protein (19,33), one prior to our work (in 2005), and the other in 2014 during the course of our studies on AGPAT4, results were ambiguous. The study by Lu *et al.* (2005) failed to find AGPAT activity for APGAT4 in COS-7 cells although the authors did detect it in reticulocyte lysates (19), while the report by Eto *et al.* (2014) may have excluded the major acyltransferase activity of this enzyme by failing to investigate activity in the mitochondrial fraction, or activity with lysophospholipid acceptors other than LPA (33). Based on high sequence homology to other members of the AGPAT superfamily, it seemed highly likely that AGPAT4 would localize to the endoplasmic reticulum and function in phospholipid synthesis and remodeling (Table 2). Prior to our work, however, it had not yet been determined experimentally what specific activity AGPAT4 had, or where it localized within cells or within the brain. At the initiation of this project, we believed that AGPAT4 could be a lysophosphatidic acid acyltransferase (LPAAT), a lysophosphatidylcholine acyltransferase (LPCAT), a LPEAT, a lysophosphatidylserine acyltransferase (LPSAT), a lysophosphatidylinositol acyltransferase (LPIAT), a lysophosphatidylglycerol acyltransferase (LPGAT), an acyl-CoA:lysocardiolipin acyltransferase (ALCAT), a GPAT, or have a combination of these functions. We also believed that it could have microsomal, mitochondrial, nuclear, or some other subcellular localization. A role in lipid biosynthesis suggests that this enzyme would be down-regulated during fasting, which is a predominantly catabolic state.

Objectives

The objectives of my thesis were to characterize AGPAT4 tissue expression, subcellular localization, and *in vitro* and *in vivo* activity, and to perform preliminary investigation of a physiological role for this enzyme by determining expression at various embryonic timepoints and during changing nutritional states.

My first objective was to determine the expression of AGPAT4 at the tissue level. *Agpat4* mRNA from a variety of murine tissues was assessed for predominate expression, and immunohistochemistry was used to detect AGPAT4 in a mixed primary neural cell culture.

My second objective was to determine the predominate localization of this enzyme at the subcellular level. This was determined by fluorescence microscopy of HEK-293 cells overexpressing an AGPAT4-GFP chimera, and was confirmed by immunoblot analysis of fractionated mouse brain assessing endogenous AGPAT4.

My third objective was to assess the biochemical activity of AGPAT4. Protein lysates from Sf9 cells overexpressing AGPAT4 were reacted with a variety of lysophospholipid acceptors in the presence of a mixture of unlabeled and radiolabeled fatty acyl-CoAs in a radiochemical enzyme assay performed *in vitro*. *In vivo* activity was assessed by gas chromatography (GC) quantification of fatty acids in specific phospholipid species resolved by thin layer chromatography (TLC) from Sf9 cells overexpressing AGPAT4.

My fourth objective was to investigate potential developmental and physiological roles for AGPAT4 by quantification of gene expression during different murine embryonic stages (E10.5, E14.5, E18.5), and in varying nutritional states (non-fasted, fasted, and refed) in a variety of murine tissues.

Hypotheses

The hypotheses of this study were:

1. AGPAT4 is an acyl-CoA-dependent lysophospholipid acyltransferase.
2. AGPAT4 will be most highly expressed in the brain.
3. AGPAT4 will localize to the endoplasmic reticulum.
4. AGPAT4 gene expression will be down-regulated during the fasted metabolic state as compared to the non-fasted and refed states.
5. AGPAT4 gene expression will be up-regulated during early murine embryogenesis.

Chapter Four – Methods

Animals

Three to four-month old female C57B/6 mice were housed in a temperature and humidity controlled environment, on a 12:12 hour reversed light/dark cycle. Where possible, littermates were used. Standard rodent chow was provided *ad libitum* unless otherwise specified (i.e. metabolic experiments). All animal procedures were approved by the University of Waterloo Animal Care Committee.

Cloning of Full-length AGPAT4 cDNA, AGPAT4-GFP, and Generation of AGPAT4 Baculovirus and Protein in Sf9 Cells

Full length murine AGPAT4 was amplified by PCR from mouse whole brain cDNA with the addition of BglII and SalI restriction sites to the N-terminal and C-terminal ends, respectively, using the following primers: forward 5'-AGA TCT ACC ATG GAC CTC ATC GGG CTG-3' and reverse 5'-CGT CGA CTT GTC CGT TTG TTT CCG TTT G-3'. The resulting amplicon was subcloned into pGEM-T-Easy resulting in production of pGEM-AGPAT4 that was verified by direct sequencing, and was then cut with BglII/SalI restriction enzymes for directional subcloning into pEGFP-N1 in frame with green fluorescent protein (GFP). Baculovirus was generated using the Bac-to-Bac® Baculovirus Expression System. A full length AGPAT4 amplicon with a C-terminal 6 x His tag and BglII and SalI restriction sites at the N-terminal and C-terminal ends was produced by PCR using 50 ng of pGEM-AGPAT4 as template and the following primers: forward 5'-AGA TCT ACC ATG GAC CTC ATC GGG CTG-3'; reverse 5'-GTC GAC GTG GTG GTG GTG GTG GTG GTC CGT TTG TTT CCG TTT GTT GTC G-3'. The resulting amplicon was subcloned into pGEM-T-Easy for direct sequencing, forming pGEM-AGPAT4-6His. This vector was subsequently digested using NotI/SalI to release full-

length AGPAT4 that was subcloned into NotI/SalI restriction sites in pCMV-3Tag-3A, which was then digested with KpnI/NotI releasing full-length AGPAT4 that was subcloned in frame with the 3x HA tag into pFastBacI. pFastBacI-AGPAT4 was transformed into DH10Bac chemically competent cells and plated on triple selection (Kanamycin, Gentamicin, Ampicillin) LB plates treated with Xgal and IPTG. Positive white colonies were prepped, verified by direct sequencing, and transfected into Sf9 cells grown in Sf-900 III media, and incubated for 3-4 days to generate baculovirus. Control baculovirus was produced by the same method but using pFastBacI without DNA insertion into the multiple cloning site. Amplified baculovirus was titred by serial dilution in cultures of Sf9 cells grown in 6-well plates, and harvested at 70-80% viability indicated by staining a subset of cells with trypan blue visualized by light microscopy. Infected Sf9 cells were harvested, and lysed in Lysis Buffer 1 (100mM Tris-HCl, pH 7.4, 5mM NaCl, 3mM $MgCl_2$) by sonication on ice (65% output, 3 x 6 s), which efficiently disrupts mitochondria and other organelles. Unbroken cells and organelles, and cellular debris were cleared by centrifugation (10,000 × g for 10 min). This process will pellet any remaining unbroken mitochondria, but not submitochondrial particles generated by sonication. Protein in supernatants was quantified using Bradford assay solution and diluted to 1 μg/μL for use in radiochemical assays or western blotting.

Cell Culture and Primary Neural Culture

HEK-293 cells were maintained in Dulbecco's Modified Eagle's Medium (DMEM) containing 10% fetal bovine serum (FBS) and 1% penicillin-streptomycin, and routinely subcultured upon reaching 90% confluence by trypsinization with 0.25% trypsin-EDTA. For primary neural cultures, fetal mice at embryonic d17.5 – 18.5 were decapitated

in a cell culture dish on ice containing dissection media (HBSS with 30mM HEPES, 0.6% w/v glucose, 2% w/v sucrose, final pH 7.4). Brains were dissected out and transferred to a 15 mL conical tube, washed 3 × with ice-cold dissection media, and the cortex was separated then incubated with 2 mL of pre-warmed 0.25% trypsin-EDTA for 20 minutes at 37°C in a humidified cell culture incubator with 5% CO_2. Post incubation, cells were spun at 1000 × g for 5 min, trypsin was removed, and samples were washed once with warm dissection media. Brain samples were then re-suspended by pipetting in 2 mL of warm plating media (DMEM/F12 + 10% horse serum + 10% FBS + 1% penicillin-streptomycin) until a homogenous mixture was achieved. The homogenate was strained using a 100 μm nylon cell strainer into a 50 mL conical tube, and centrifuged at 1000 × g for 5 minutes at 4°C. The pellet, containing mixed cortical neurons and glial cells, was re-suspended in 2 mL of plating media, and cells were seeded onto glass coverslips pretreated with poly-D-lysine and incubated at 37°C with 5% CO_2 for 3 hours. Once cells had attached to the plate, 50% of plating media was removed, and supplemented with feeding media (Neurobasal media + 1% B27 supplement) to support the differentiation of primary neurons.

RNA Extraction, Reverse Transcription (RT) PCR, and RT qPCR

Whole-embryos and mouse organs were collected and flash frozen in liquid nitrogen at the Central Animal Facility at the University of Waterloo. Total RNA was isolated from tissues using TRIzol® Reagent (1 mL/≤100 mg tissue) and a Polytron® homogenizer (VWR, Radnor PA) set at the highest speed. Samples were then incubated at room temperature for 5 minutes, followed by the addition of chloroform (20% of TRIzol® volume) with vigorous shaking for 15-20 seconds, incubation at room temperature for 2

minutes, and centrifugation at 12,000 x g for 15 minutes at 4°C. The upper aqueous phase of each sample was removed and mixed with isopropanol (50% of initial volume of TRIzol®), and incubated at room temperature for 10 minutes to precipitate the RNA. Samples were then centrifuged at 12,000 x g for 10 minutes at 4°C, pelleting the RNA. The supernatant was discarded and the pellet was washed in 1 mL of 75% ethanol-25% DEPC water, centrifuged at 7,500 x g for 5 minutes at 4°C, then air-dried for 5-10 minutes prior to suspension in 50 μL DEPC-ddH_2O. The solution was then incubated at 58°C for 12 minutes to facilitate solubilization, and stored long-term at -80°C. RNA samples were quantified using a Nanodrop 2000 Spectrophotometer (Thermo Scientific, Waltham MA), and samples were adjusted to 2 μg/μL. cDNA was synthesized from 2 μg of RNA by oligo(dT) priming using SuperScript II Reverse Transcriptase according to the manufacturer's protocol. Briefly, 2 μg of RNA was mixed with 1 μL of 10 mM dNTPs and 1μL of oligo$(dTs)_{12-18}$ and incubated at 65°C for 5 minutes in a denaturation step, cooled briefly on ice (1-2 minutes), then mixed with 6 μL of reaction mix (consisting of 4 μL of 5X first strand buffer, 2 μL 0.1M DTT) and incubated at 42°C for 2 minutes to allow for primer annealing. Finally, 80 units of Superscript II Reverse Transcriptase were added to each sample and cDNA synthesis was allowed to proceed at 42°C for 50 minutes with termination of reactions by incubation at 70°C for 15 minutes. cDNA was stored at -80°C. Tissue-specific expression of *Agpat4* was determined using 1 μL of cDNA amplified by PCR using the primers: forward *Agpat4* 5'-ATG GAC CTC ATC GGG CTG CTG-3', reverse *Agpat4* 5'- GTC CGT TTG TTT CCG TTT GTT GTC G-3' (1133 bp amplicon) and forward *36B4* 5'-CAG CAG GTG TTT GAC AAC GG-3', reverse *36B4* 5'-TGG TTG CTT TGG CGG GAT TA-3' (404 bp amplicon) or by Taqman gene expression

assays (Mm00509777_m1 for *Agpat4* and Mm04277571_s1 for *18S*) in a CFX-96 Connect Real Time PCR Detection System (BioRad, Hercules CA). The thermal cycling protocol was as follows: One cycle of 95°C for 5 minutes, 40 cycles at 95°C for 15 seconds, then 60°C for 30 seconds. Gene expression levels were normalized to *18S* and quantified by the ΔΔCt method.

In vitro acyl-CoA:lysophospholipid acyltransferase assay and thin layer chromatography

A substrate mixture containing 80 μM lysophospholipid, 200 μM oleoyl-CoA, and [^{14}C]oleoyl-CoA (0.025 μCi per reaction) was prepared, dried under a stream of N_2 and reconstituted in reaction buffer (100 mM Tris, pH 7.0, 4 mg/mL BSA) by vortexing at high speed for 30 s. Reactions were initiated by addition of 100 μL of pre-warmed substrate mixture to 100 μL of sonicated, cleared lysates from Sf9 cells infected with either AGPAT4 or control baculovirus, prepared as described above. Reactions were mixed gently, and incubated in a 37°C water bath for 30 min, then quenched by addition of 0.75 mL of methanol:chloroform (2:1, v/v). Lipids were extracted by the method of Bligh & Dyer (35). Briefly, quenched reactions were mixed with 0.25 mL of chloroform, vortexed thoroughly, mixed with 0.25 mL of ddH_2O, vortexed again, then centrifuged at 1000 × g for 5 minutes to separate aqueous (upper) and organic (lower) phases. The organic phase was recovered and dried under a stream of N_2. Samples were reconstituted in 50 μL of chloroform, applied to a silica gel G plate, and resolved by TLC using a hexane:diethyl ether:glacial acetic acid solvent system (80:20:2, v/v/v). The band corresponding to phospholipids was scraped and extracted from silica by the addition of 0.75mL of methanol:chloroform, upon which a further lipid extraction by the method of Bligh & Dyer followed. The organic phase was recovered and dried under a stream of N_2.

Samples were reconstituted in 50 μL of chloroform, applied to a silica gel H plate, and resolved by polar lipid TLC using a chloroform:methanol:2-propanol:0.25% KCl:triethylamine solvent system (30:9:25:6:18, v/v/v/v/v). Phospholipid species were identified by known standards, and corresponding bands were scraped and quantified by liquid scintillation counting.

In vivo phospholipid fatty acid analysis

Sf9 cells grown in 250 mL flasks were infected with either control or AGPAT4 baculovirus. Seventy-two hours later, cells were harvested by gentle aspiration into 50 mL concial tubes. A subset of the cells (1 mL) was lysed for extraction and quantification of protein, while another subset (1 mL) was extracted by the method of Folch using 2:1 (v/v) chloroform:methanol with butylated hydroxytoluene as an antioxidant (Sigma-Aldrich, Bellfonte PA), and subsequent addition of sodium phosphate (36). The organic phase was applied to a silica gel H plate and resolved by TLC on a chloroform:methanol:2-propanol:0.25% KCl:triethylamine solvent front (30:9:25:6:18, v/v/v/v/v). Bands corresponding to individual phospholipid species were identified using known standards, overlaid with 10 μg of 22:3n-3 ethyl ester internal standard (Nu-Check Prep, Elysian, MN), and scraped for determination of fatty acid composition and content by gas chromatography with flame ionization detection as previously described (37). Briefly, fatty acid methyl esters were derivatized by transesterification using 14% boron trifluoride in methanol (Thermo Scientific, Bellfonte PA) with hexane on a 95°C heat block for 1 h. Fatty acid methyl esters were analyzed on a Varian 3900 gas chromatograph equipped with a DB-FFAP 15 m x 0.10 mm injected dose x 0.10 μm film thickness, nitroterephthalic acid modified, polyethylene glycol, capillary column (J&W Scientific

from Agilent Technologies, Mississauga, Ontario, Canada) with hydrogen as the carrier gas. Samples (2 μL) were introduced by a Varian CP-8400 autosampler into the injector heated to 250°C with a split ratio of 200:1. Initial temperature was 150°C with a 0.25-minute hold followed by a 35°C/minute ramp to 200°C, an 8°C/minute ramp to 225°C with a 3.2-minute hold, and then an 80°C/minute ramp up to 245°C with a 15-minute hold at the end. The flame ionization detector temperature was 300°C with air and nitrogen make-up gas flow rates of 300 and 25 mL/min, respectively, and a sampling frequency of 50 Hz (37).

Subcellular fractionation

Subcellular fractions were separated as previously described (38), with minor modifications. Briefly, mouse brains were harvested and homogenized at 1,000 rpm in buffer A (250 mM Sucrose, 50 mM Tris-HCl, pH 7.4, 5 mM $MgCl_2$), then centrifuged at 800 × g for 15 min to isolate the nuclear fraction. All centrifugation steps were performed at 4°C. Post-nuclear supernatants were removed to a fresh tube on ice for further processing. The nuclear pellet was washed twice by re-suspending in 300 μL of buffer A, with added protease and phosphatase inhibitor cocktails, followed by 15 min centrifugations at 500 × g, then 1000 × g. The final pellet was re-suspended in 300 μL of buffer B (20 mM HEPES pH 7.9, 1.5 mM $MgCl_2$, 0.5 M NaCl, 0.2 mM EDTA, 20% (v/v) glycerol, and 1% Triton X-100), incubated on ice for 30 min, then sonicated into homogenous suspension while held in an ice bath using three pulses at 65% output for 6 s with a 30 s cooling period in between pulses. Sonicated nuclei were spun at 9000 × g for 30 min to pellet debris, and the supernatant containing the nuclear fraction was recovered. Post-nuclear supernatants from the initial lysis and centrifugation of cells were spun at

11,000 × g for 10 min to pellet mitochondria. The post-mitochondrial supernatant was removed to a fresh tube and centrifuged for 1 h at 100,000 × g to isolate the microsomal fraction, following which the cytosolic supernatant was discarded, and the pellet was re-suspended in 50 μL of buffer C (50mM Tris-HCl, pH 6.8, 1 mM EDTA, and 0.5% Triton X-100) by brief suspension of tubes in an ice-cold sonicating water bath. The mitochondrial pellet was resuspended in 100 μL of buffer C and sonicated with three 6 s bursts at 65% output in an ice water bath, with a 30 s cooling period between pulses.

Immunoblotting

Protein lysates were mixed with 2 × Laemmeli Buffer (125 mM Tris-HCl, pH 6.8, 20% glycerol, 4% SDS, 10% 2-mercaptoethanol, and 0.05% bromophenol blue) and denatured by heating to 95°C for 5 min. Samples were electrophoresed on 12% SDS-PAGE gels at 100V for 1 h, and transferred to nitrocellulose membranes at 350A for 90 minutes to be used for immunodetection. Membranes were blocked for 1 h with 5% skim milk powder (w/v) in TBST (50 mM Tris-HCl, pH 7.4, 150 mM NaCl, 0.1% Tween-20), then probed overnight in TBST with 1% skim milk powder (w/v) using primary antibodies (1:1000 dilution) directed against AGPAT4 (Sigma Aldrich, St. Louis MO), CYTOCHROME C, SCD1 (Cell Signalling, Beverly MA), or HISTONE H3 (EMD Millipore, Billerica MA). Bands were detected by incubation of blots with HRP-conjugated anti-mouse or anti-rabbit secondary antibodies followed by enhanced chemiluminescence.

Immunofluorescence

For studies on subcellular localization, HEK-293 cells were grown on coverslips, then transfected with pEGFP-N1 (control vector) or chimeric pEGFP-AGPAT4, with or

without pDSRed2-Mito (Life Technologies, Carlsbad CA), using Lipofectamine® 2000 according to the manufacturer's instructions. Forty-eight hours later, cells that were not transfected with pDsRed2-Mito were stained with ER-Tracker™ Red (Life Technologies, Carlsbad CA) diluted 1:10,000 in Hank's Buffered Salt Solution (HBSS), pH 7.1, for 30 min at 37°C and 5% CO_2. Cells were washed twice with HBSS and fixed with 4% paraformaldehyde for 10 min, then nuclei were counter-stained with 1 μg/mL diamidino-2-phenylindole (DAPI) for 15 minutes. Samples were washed again in PBS prior to mounting on glass microscope slides using Prolong Antifade mounting medium (Life Technologies, Carlsbad CA). Cells were visualized with an Axio Observer Z1 microscope equipped with Axio Cam HRm camera and Axiovision Software (Carl Zeiss).

Primary embryonic neurons and glial cells were isolated and grown on coverslips pretreated with poly-D-lysine, then fixed with 4% paraformaldehyde for 10 min, washed with PBS, and permeabilized with 0.5% Triton X-100 for 5 min at room temperature. Cells were then washed with PBS and blocked with 5% goat IgG serum in PBS. After 1 h, blocking serum was removed, and cells were incubated at room temperature for an additional hour with rabbit anti-AGPAT4 antibody (Bioss, Woburn MA), diluted 1:100 in PBS, alone or in combination with mouse anti-GFAP (1:500 dilution) or mouse anti-NESTIN antibodies (1:500 dilution) (Cell Signaling, Danvers MA). Cells were then washed with PBS, and incubated for 1 h at room temperature with Alexa Fluor® 555-conjugated anti-rabbit IgG, and/or Alexa Fluor® 488-conjugated anti-mouse IgG (Cell Signaling, Danvers MA), or stained with Neurotrace® 500/525 Green Fluorescent Nissl Stain (1:100 dilution in PBS) for 20 min at room temperature according to the

manufacturer's protocol (Life Technologies, Carlsbad CA). Cells were then washed repeatedly with 0.1% Triton X-100 in PBS followed by PBS alone, stained with DAPI (1 μg/mL) for 15 min, and mounted on glass microscope slides using Prolong Antifade.

Statistical Analysis

The results are expressed as means ± S.E.M. Statistically significant differences between two groups were assessed by Student's *t* test. Differences between multiple groups were assessed by one-way analysis of variance with Bonferroni's post hoc test. Significance is accepted at $P < 0.05$.

Chapter Five – Results

Agpat4 is highly expressed in brain

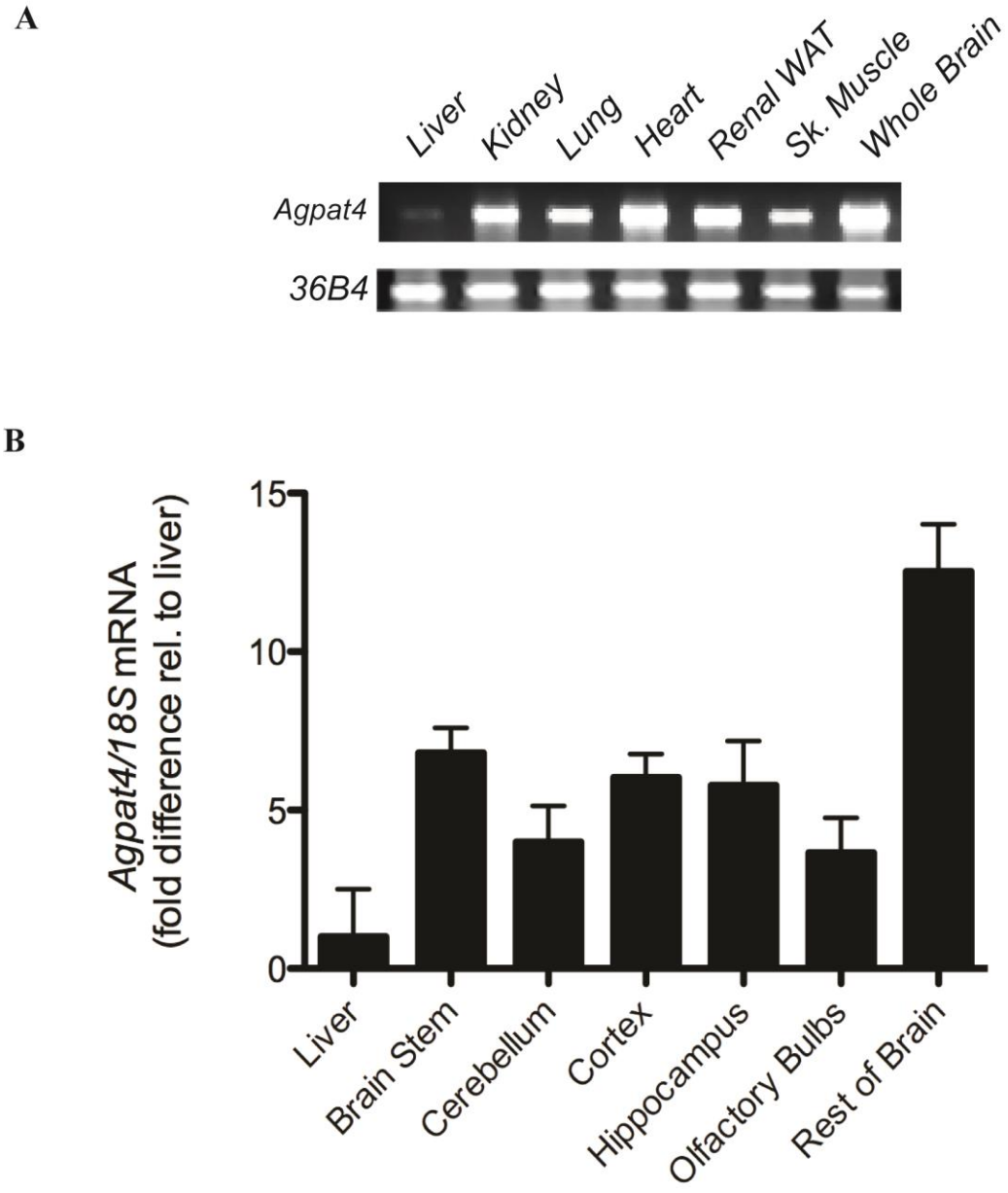

Figure 4: AGPAT4 is highly expressed in multiple brain regions. *A,* representative ethidium bromide agarose gel showing AGPAT4 mRNA expression measured by RT-PCR in multiple tissues including whole brain. *B,* AGPAT4 mRNA expression determined by qPCR in multiple regions of the central nervous system (n-3).

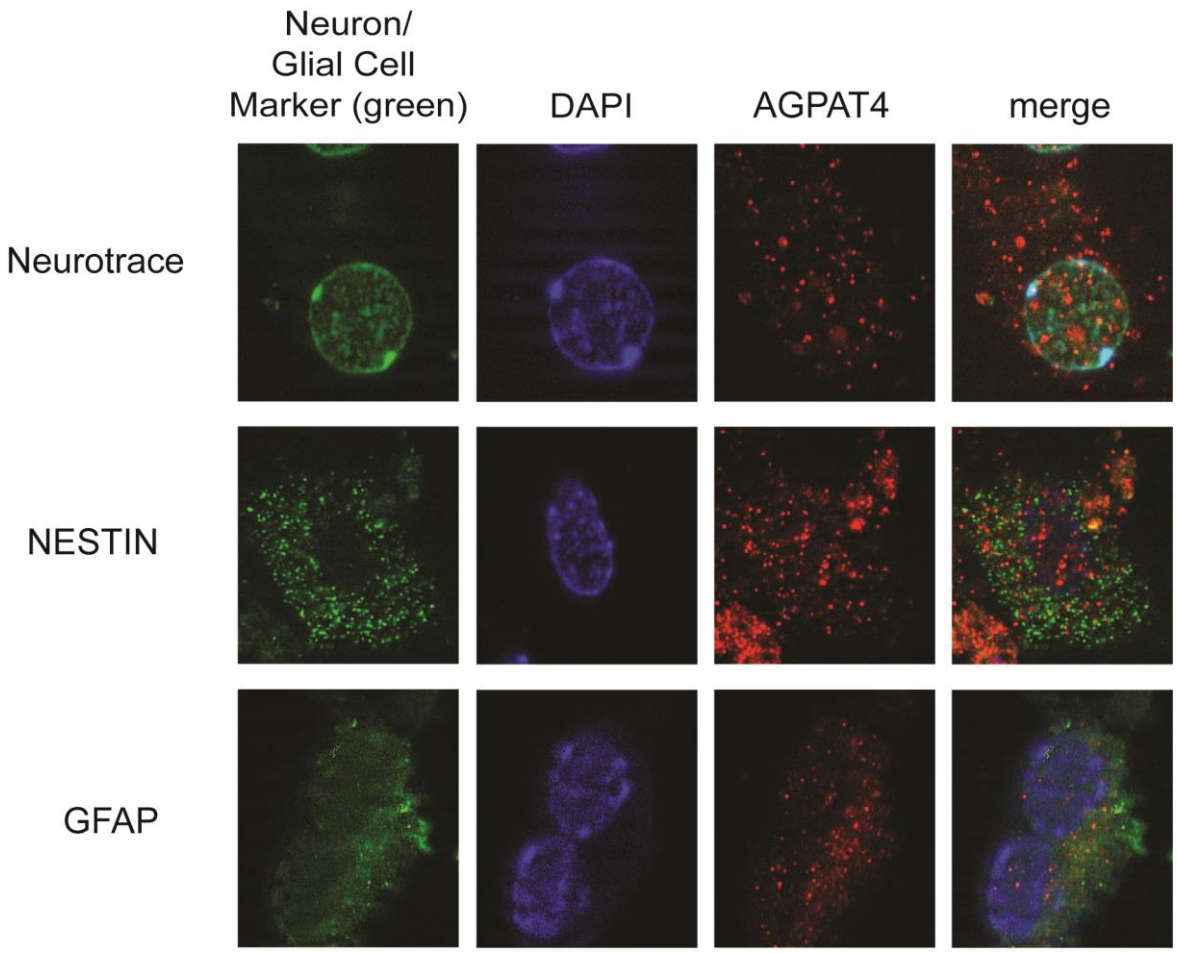

Figure 5: AGPAT4 is highly expressed in neuronal and astroglial cells. Representative images showing immunodetection of AGPAT4 in cultured primary cortical neurons and glial cells. Primary neurons were identified by positive detection of the neuron-specific protein NESTIN, or by co-staining with green fluorophore-labeled Nissl stain. Astroglial cells were identified by the detection of the glial marker GFAP.

The tissue distribution of *Agpat4* mRNA was analyzed and, as expected (19,25,33), was found to be highly expressed in mouse whole brain homogenates (Fig. 4*A*). *Agpat4* was also present at variable levels in all other tissues examined including liver, kidney, lung, heart, renal white adipose tissue (WAT), and skeletal muscle. Dissection of mouse brains to isolate olfactory bulbs, hippocampus, cerebellum, cortex, brain stem, and the remaining brain tissue, followed by RNA preparation and RT-qPCR analysis indicated only a small variation in *Agpat4* expression within major regions of the central nervous system, with no significant differences between regions (Fig. 4*B*).

To determine whether AGPAT4 is expressed in neurons or in glial cells, or in both cell types, we performed immunohistochemistry on mixed cultures of primary cortical neural cells derived from brains of d18.5 embryonic mice. Cells were grown on coverslips for 7 days in Neurobasal® medium with B27 supplementation to promote neuronal differentiation. Primary neurons were identified as cells expressing the neuron-specific intermediate filament NESTIN, or cells positively co-staining with the fluorescent green Nissl stain Neurotrace 500/525®. Glial cells were identified as cells expressing glial fibrillary acidic protein (GFAP). AGPAT4 showed a diffuse, punctate staining (Fig. 5), and was found to co-localize in cells that were identified as positive for either Nissl stain or immunodetectable NESTIN, indicating the presence of this enzyme in primary cortical neurons (Fig. 5). AGPAT4 was also detected, albeit at a somewhat lower intensity, in cells that co-expressed GFAP, indicating that is also found in astroglial cells.

AGPAT4 localizes to the mitochondria

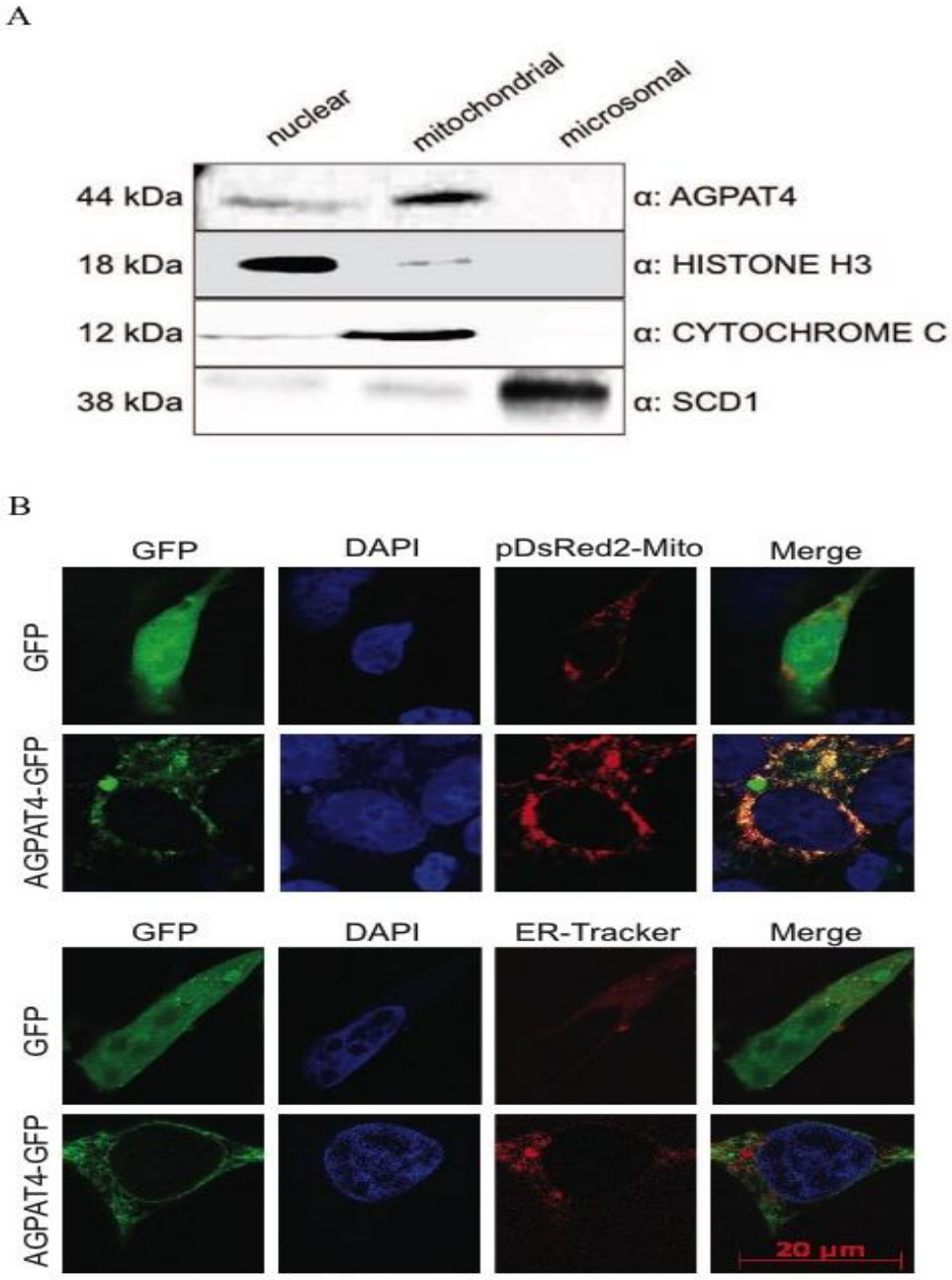

Figure 6: AGPAT4 localizes predominately to the mitochondria. *A*, Mouse brains were harvested and subjected to differential centrifugation to separate nuclear, mitochondrial, and microsomal fractions. Purity of the fractions was determined by immunoblotting for markers of mitochondria (CYTOCHROME C), endoplasmic reticulum (SCD1), and nuclei (HISTONE H3). *B*, HEK-293 cells were transfected with pEGFP-N1 (control) or AGPAT4 and co-transfected with pDsRed2-Mito, or stained with ER Tracker™ Red dye, then imaged by confocal microscopy.

To determine the predominant subcellular localization of AGPAT4, mouse brains were harvested and subjected to differential centrifugation. Immunoblot analysis for AGPAT4 indicated predominate detection of this protein in the mitochondrial fraction (Fig. 6), with a faint band apparent in the nuclear fraction, but essentially no AGPAT4 detectable in the microsomal fraction. Fractional purity was assessed by immunoblotting for the mitochondrial protein CYTOCHROME C, the nuclear protein HISTONE H3, and SCD1 that is expressed in the endoplasmic reticulum, but not in the mitochondria.

The subcellular localization of AGPAT4 was further investigated in HEK-293 cells transfected with pEGFP-N1 (control plasmid) or pEGFP-*Agpat4*. To coordinately visualize the endoplasmic reticulum or mitochondria, transfected cells were either stained with ER Tracker ™ Red dye, or co-transfected with the mitochondria localization plasmid pDsRed2-Mito, respectively. Imaging by confocal microscopy indicated that AGPAT4-GFP in HEK-293 cells displayed a diffuse, punctate distribution (Fig. 6*B*) that was similar to immunodetectable AGPAT4 in primary neurons and glial cells (Fig. 5). Although AGPAT4-GFP predominately displayed an extra-nuclear localization, an increased intensity of green fluorescence was evident around the nucleus compared to the cytoplasm suggesting, in agreement with data from differential centrifugation (Fig. 6*A*), that a small fraction of AGPAT4 may localize, at least in part, to the nuclear membrane. Subcellular visualization of green fluorescent AGPAT4 based on coordinate imaging with either red fluorescent pDsRed2-Mito or ER Tracker ™ Red indicated that this enzyme predominately localizes to the mitochondria and not to the endoplasmic reticulum (Fig. 7*B*). Analysis of the extent of co-localization using MIPAV (v7.0.1) software

demonstrates 86% co-localization between AGPAT4-GFP and pDsRed2-Mito, but only 8% co-localization between AGPAT4-GFP and ER Tracker ™ Red. Transfection of cells with pEGFP-N1 alone led to a diffuse fluorescence throughout all areas of the cell.

AGPAT4 has acyl-CoA:lysophosphatidic acid acyltransferase (LPAAT) activity in vitro

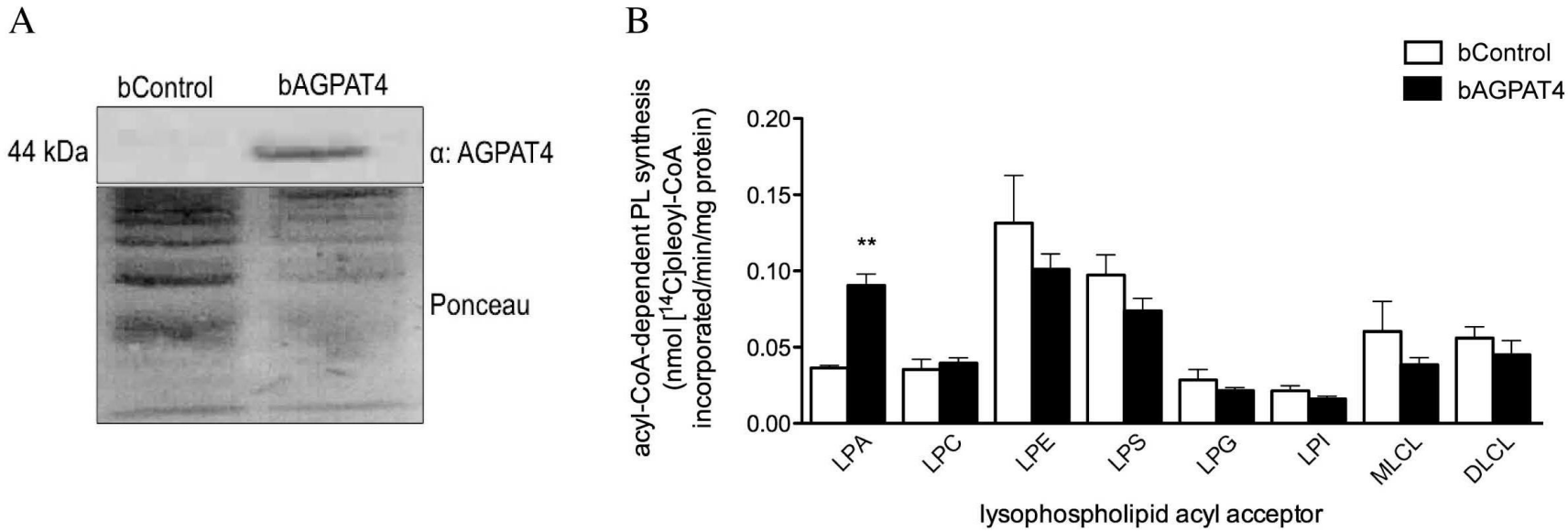

Figure 7: AGPAT4 is an acyl-CoA:lysophosphatidic acid acyltransferase *in vitro*. *A*, Immunoblot of Sf9 cells overexpressing AGPAT4. *B*, Protein lysates from Sf9 cells infected with either control or AGPAT4 baculovirus were assayed *in vitro* for acyl-CoA-dependent lysophospholipid acyltransferase activity using [^{14}C]oleoyl-CoA and a variety of lysophospholipid acyl acceptors. Bands corresponding to individual phospholipid species were quantified by liquid scintillation counting (n=3-4) (*C*). **P<0.01 vs. control.

To determine the activity of AGPAT4 *in vitro*, we produced cell lysates from Sf9 cells overexpressing AGPAT4 (Fig. 7*A*). Sequence analysis of AGPAT4 indicated the presence of conserved motifs that are common to the AGPAT family of enzymes (Table 2) leading us to initially investigate possible acyl-CoA-dependent lysophospholipid acyltransferase activities for this enzyme. We utilized [oleoyl-1-^{14}C]-CoA as the acyl donor, and a variety of common lysophospholipids as acyl acceptors including LPA, LPC, LPE, and lysophosphatidylserine (LPS). However, our finding of a predominate mitochondrial localization (Fig. 6*A,B*) suggested the possibility that AGPAT4 may be involved in remodeling mitochondria-specific phospholipids, such as phosphatidylglycerol (PG) or CL. We therefore also screened a wider panel of potential lysophospholipid acceptors including less abundant or organelle-specific lysophospholipid species such as LPG, LPI, MLCL, and DLCL. Compared to reactions performed with control lysates, reactions with lysates overexpressing AGPAT4 produced significantly more radiolabeled PA from LPA as quantified by liquid scintillation counting (Fig. 7*B*). Lysates overexpressing AGPAT4 increased esterification of [^{14}C]oleoyl-CoA into LPA by ~2.5-fold compared to control. Under our assay conditions, overexpression of AGPAT4 had no significant effect on incorporation of [^{14}C]oleoyl-CoA into LPC, LPE, LPS, LPG, LPI, MLCL, or DLCL. This profile of *in vitro* lysophospholipid acyl-acceptor specificity is highly similar to that which has been previously reported (19,33).

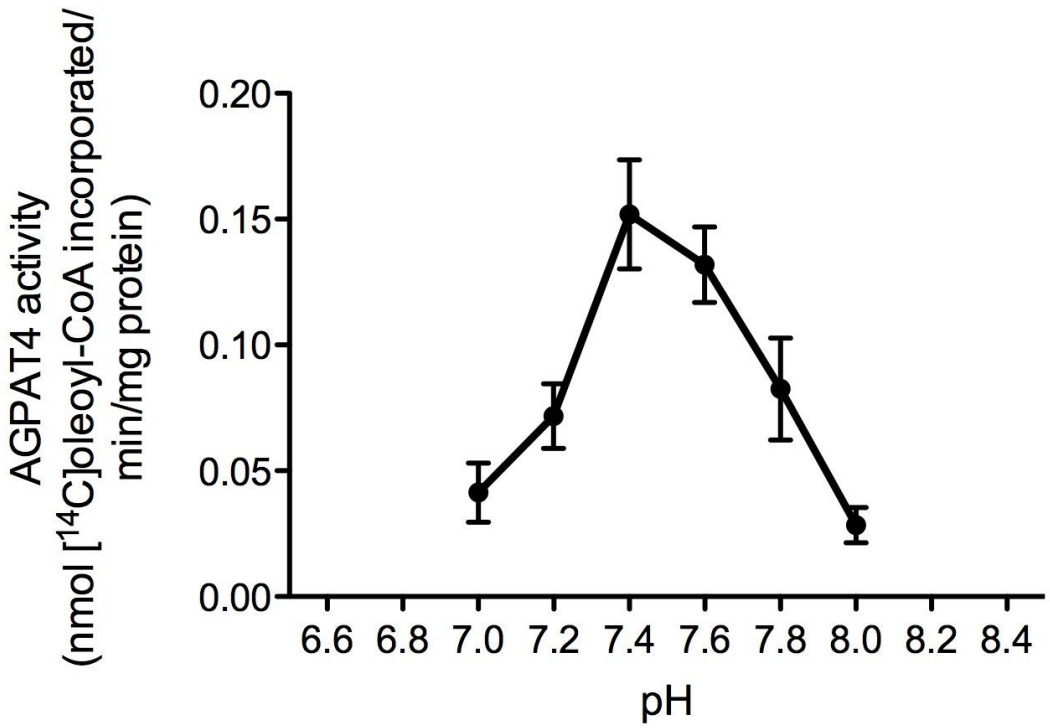

Figure 8: pH dependency of AGPAT4 activity. Protein lysates from Sf9 cells infected with either control or AGPAT4 baculovirus were assayed *in vitro* for acyl-CoA-dependent lysophospholipid acyltransferase activity using [^{14}C]oleoyl-CoA and lysophosphatidic acid at varying cellular pH. Bands corresponding to phosphatidic acid were quantified by liquid scintillation counting. Highest AGPAT4 activity was observed at pH 7.4 (n=3).

Cellular pH varies significantly across different subregions of cells, and across organellar membranes. Optimal pH of AGPAT4 enzyme activity was assessed by *in vitro* assay of [^{14}C]oleoyl-CoA:LPA acyltransferase activity in reaction buffer at varying pH levels, ranging from pH 7 to 8. We observed the highest AGPAT4 enzyme activity at pH 7.4 (Fig. 8).

AGPAT4 over expression increases the cellular content of PI

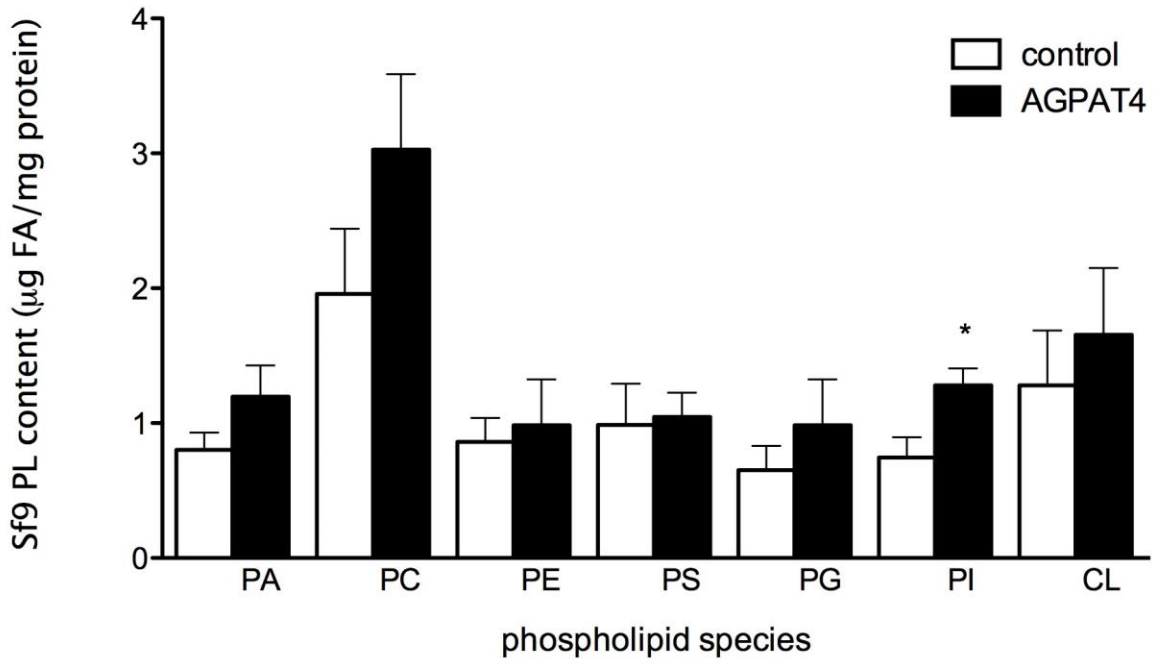

Figure 9: AGPAT4 has acyl-CoA:lysophosphatidylinositol activity *in vivo*. Endogenous phospholipids from Sf9 cells overexpressing either AGPAT4 or control vector were analyzed for fatty acyl content of different phospholipid species. Samples were grown in triplicate in three separate experiments. * $P<0.05$ vs. control.

Sf9 cells were infected with baculoviral AGPAT4 or control virus for 72 h, then harvested and extracted for total endogenous lipids. Individual phospholipids were resolved by TLC, identified by comparison with defined standards, scraped, and analyzed for fatty acyl composition and content, which was also used to calculate the corresponding cellular phospholipid levels. Cells overexpressing AGPAT4 had an ~72% greater total cellular PI content compared to control cells (37.14 ± 3.67 μg FA in PI/mg cells versus 21.62 ± 4.33 μg FA in PI/mg cells, respectively, P=0.0009) (Fig. 9). There were no other significant differences in total levels of any of the other phospholipids analyzed, including PC, PE, PG, PS, or CL.

While total cellular PA content is important for mitochondrial metabolism and cell health, the specific fatty acyl composition of PA is also of critical importance (45,64). We therefore determined and quantified the fatty acyl composition of PA from Sf9 cells overexpressing AGPAT4 and found a significant increase in the total content of two saturated fatty acyl species (Figure 10). Among individual saturated fatty acyl species, we found a significantly higher content of lauric acid (C12:0) and arachidic acid (C20:0) in PA from cells overexpressing AGPAT4 as compared to controls. There were no significant differences in PA content of any of the monounsaturated fatty acid, or n-6 or n-3 PUFA species analyzed including docosahexanoic acid (22:6-3). Although DHA appeared to be marginally higher in the AGPAT4 overexpressing group, this did not reach significance (P=0.17).

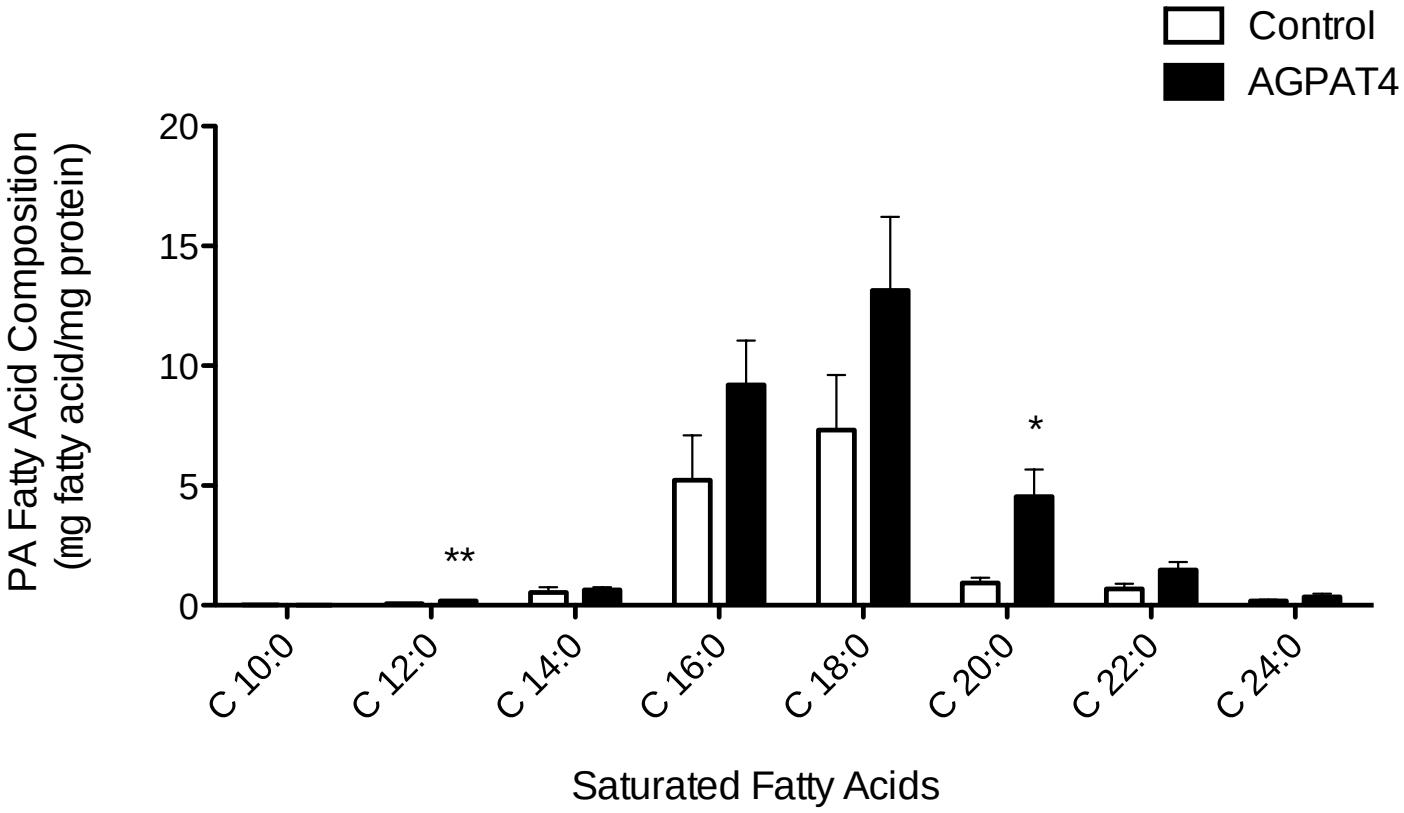

Figure 10: AGPAT4 overexpression results in higher levels saturated fatty acid species esterified in PA *in vivo*. Sf9 cells were grown in 250 mL flasks in triplicate, in three separate experiments, and infected with AGPAT4 or control baculovirus for 72 hours prior to harvest. Total lipids were extracted and resolved by TLC to isolate PA. Fatty acids in PA were identified and quantified by GC. Cells infected with AGPAT4 had in a higher level of lauric acid (171%) and arachidic acid (382%) esterified in PA as compared to controls. * $P<0.05$, ** $P<0.01$.

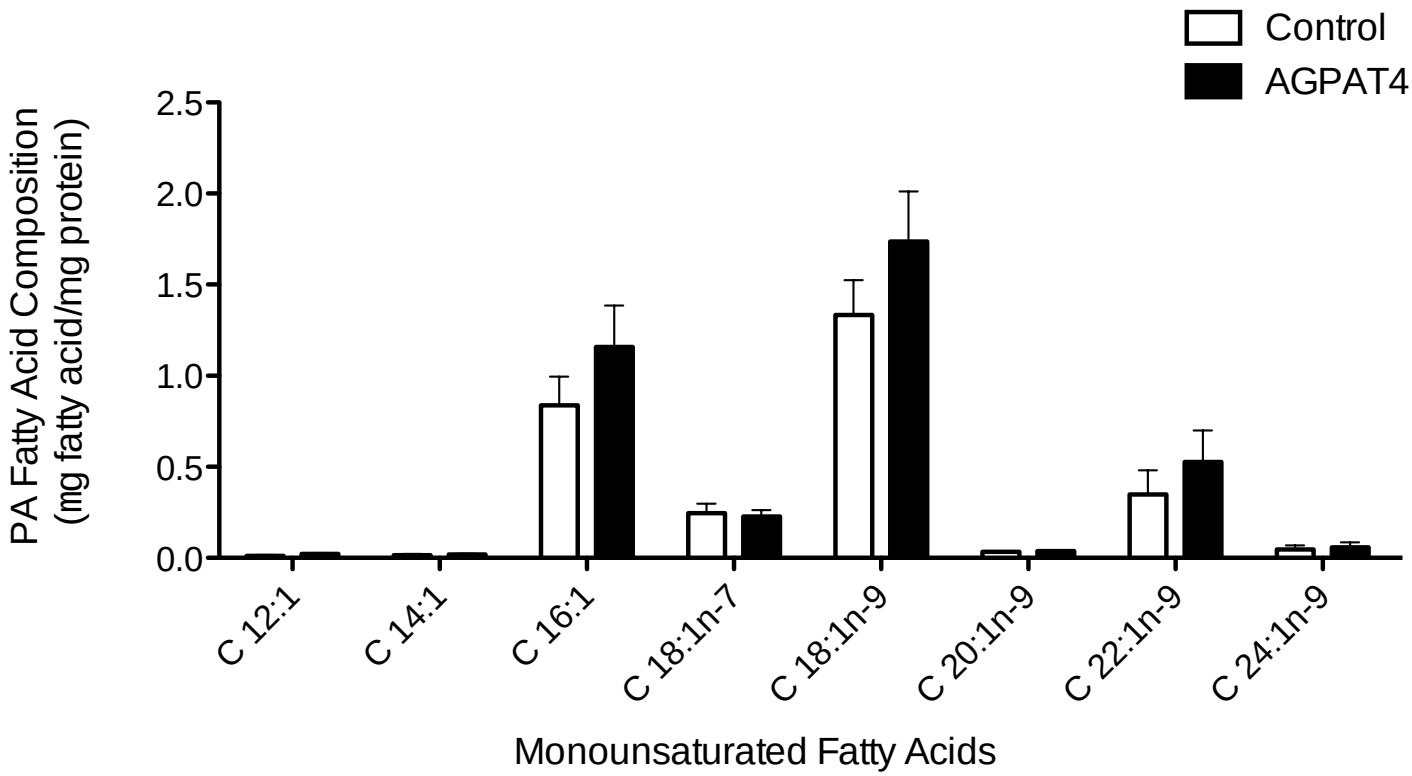

Figure 11: AGPAT4 overexpression does not result in higher levels of monounsaturated fatty acids esterified in PA *in vivo*. Sf9 cells were grown in 250 mL flasks plates in triplicate, in three separate experiments, and infected with AGPAT4 or control baculovirus for 72 hours prior to harvest. Total lipids were extracted and resolved by TLC to isolate PA. Fatty acids in PA were identified and quantified by GC. Cells infected with AGPAT4 did not result in a higher level of monounsaturated fatty acids esterified in PA as compared to controls.

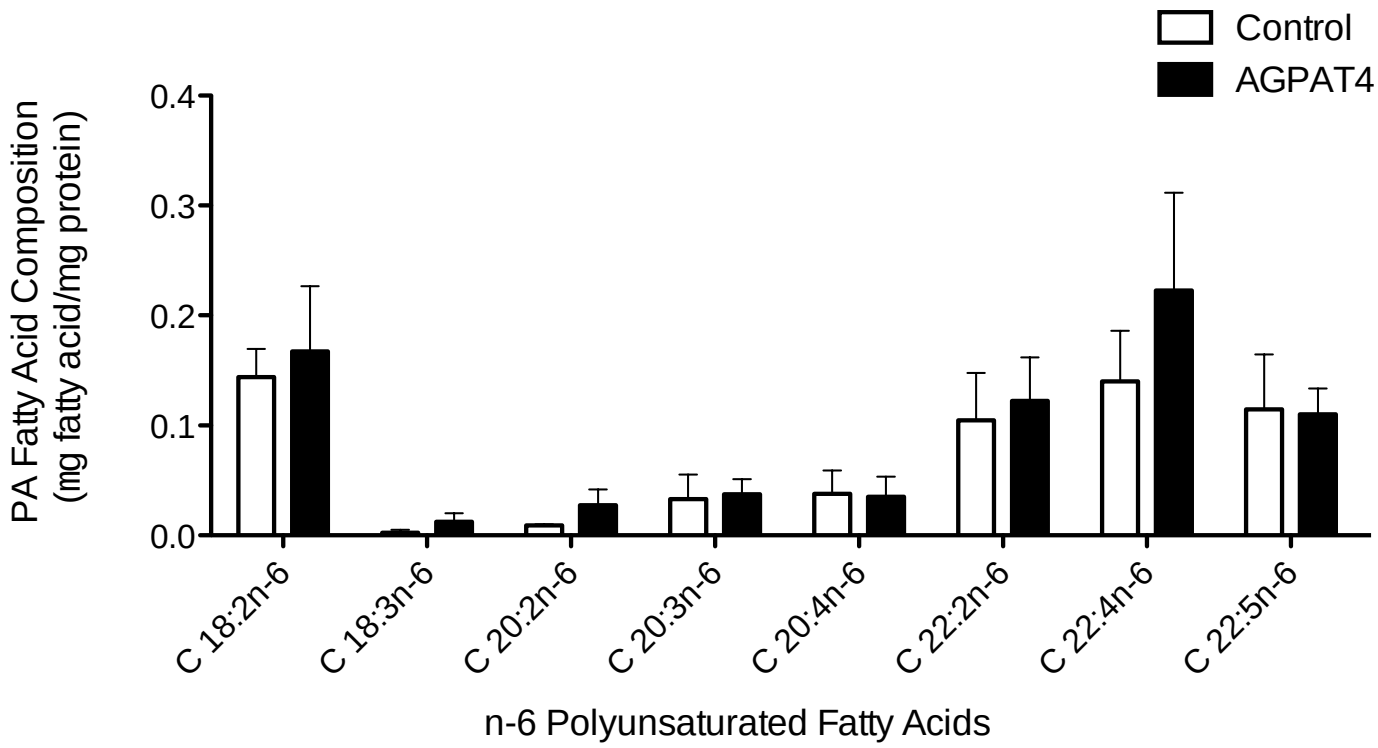

Figure 12: AGPAT4 overexpression does not result in higher levels of n-6 polyunsaturated fatty acids esterified in PA *in vivo*. Sf9 cells were grown in 250 mL flasks plates in triplicate, in three separate experiments, and infected with AGPAT4 or control baculovirus for 72 hours prior to harvest. Total lipids were extracted and resolved by TLC to isolate PA. Fatty acids in PA were identified and quantified by GC. Cells infected with AGPAT4 did not result in a higher level of n-6 polyunsaturated fatty acids esterified in PA as compared to controls.

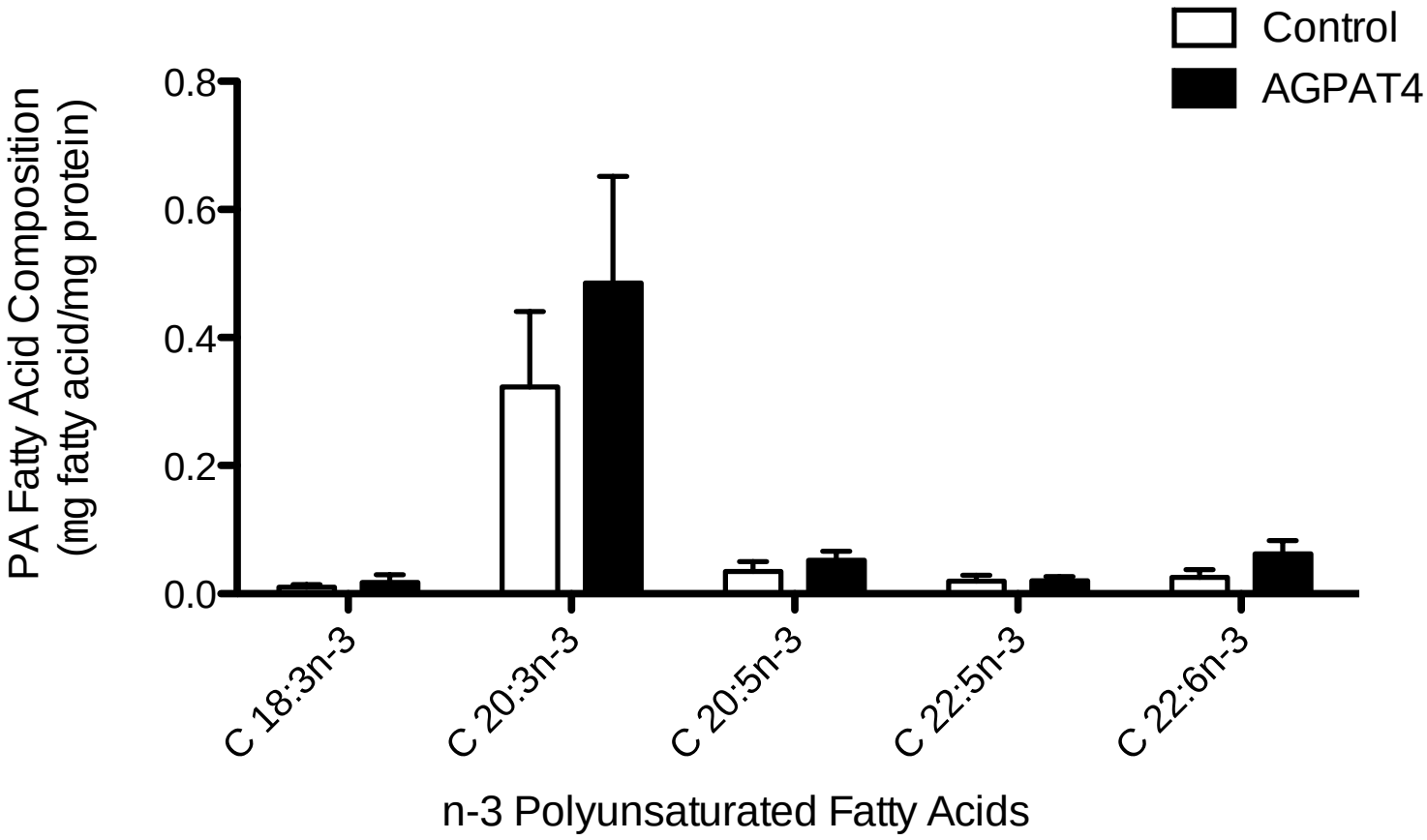

Figure 13: AGPAT4 overexpression does not result in higher levels of n-3 polyunsaturated fatty acids esterified in PA *in vivo*. Sf9 cells were grown in 250 mL flasks plates in triplicate, in three separate experiments, and infected with AGPAT4 or control baculovirus for 72 hours prior to harvest. Total lipids were extracted and resolved by TLC to isolate PA. Fatty acids in PA were identified and quantified by GC. Cells infected with AGPAT4 did not result in a higher level of n-3 polyunsaturated fatty acids esterified in PA as compared to controls.

AGPAT4 mRNA expression is developmentally and metabolically regulated

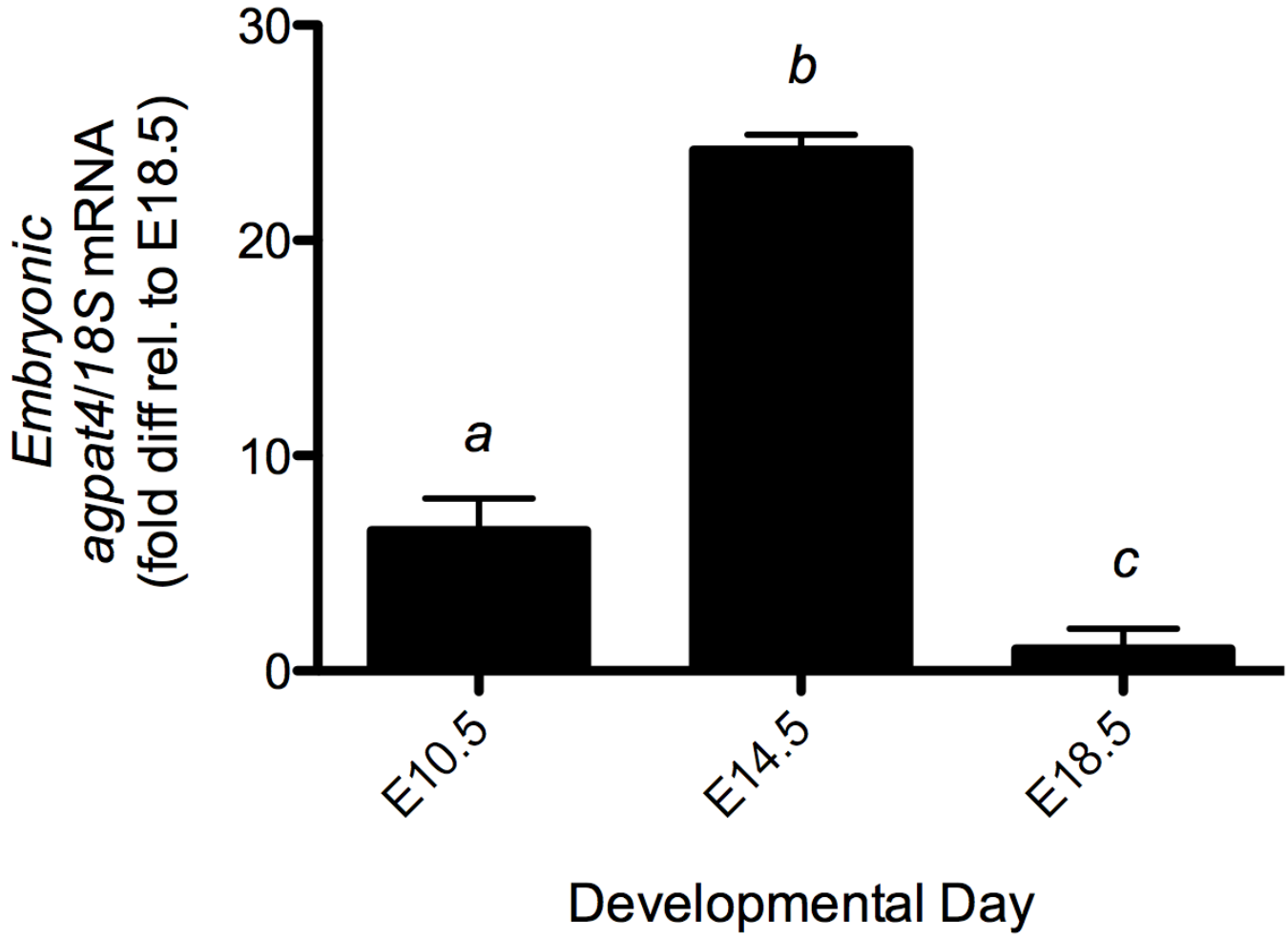

Figure 14: AGPAT4 is regulated during murine embryogenesis. AGPAT4 mRNA expression in whole mouse embryos harvested at embryonic developmental day 10.5 (mid-2nd trimester), 14.5 (end of 2nd trimester), and 18.5 (end of 3rd trimester, immediately prior to birth) (n=4-6). Data are means ± S.E.M. $^{a\ vs.\ b;\ b\ vs.\ c}$ P<0.001, $^{a\ vs.\ c}$ P<0.05.

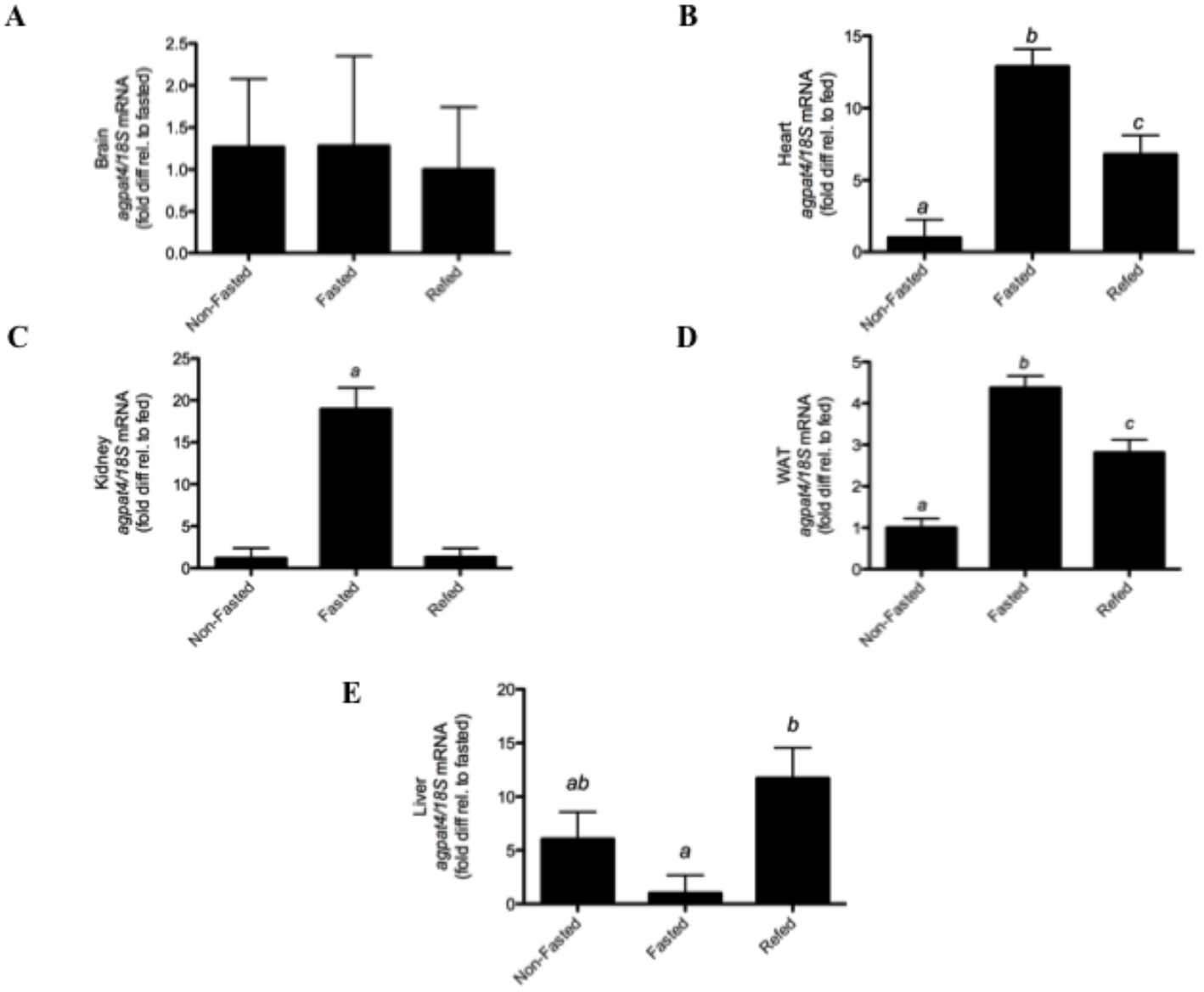

Figure 15: AGPAT4 is regulated during embryogenesis and in different metabolic states. AGPAT4 mRNA expression in various organs of mice that had access to food *ad libitum* (non-fasted), or that underwent a 16 h overnight fast (fasted), or that were fasted and then re-fed for 4 h prior to sacrifice (n=5-6) (*B-F*). Data are means ± S.E.M. $^{a\ vs.\ b;\ b\ vs.\ c}$ P<0.001; $^{a\ vs.\ c,\ d;\ b\ vs.\ d}$ P<0.05.

Embryogenesis is a time of rapid cellular and organellar growth, with high demands for mitochondrial energy metabolism. It is also a time for organogenesis, with rapid development and expansion of specialized structures such as the central nervous system. To determine whether *Agpat4* is regulated during embryogenesis, total RNA was isolated from mouse embryos on developmental days 10.5, 14.5, and 18.5, and analyzed by RT-qPCR for relative *Agpat4* expression normalized to *18s* expression (Fig. 15). *Agpat4* was upregulated 3.7-fold at developmental day 14.5 as compared to 10.5. *Agpat4* mRNA levels then decreased to only 4% of developmental day 14.5 levels immediately prior to birth, on d18.5.

Genes involved in cellular energy metabolism must also respond to changes in the availability of nutrients in order to successfully transition between states of high and low energy availability. To determine whether *Agpat4* expression is regulated in response to changing metabolic conditions, total RNA was prepared from multiple organs of mice provided with food *ad libitum* (i.e. in the non-fasted state), or subjected to a 16 h overnight fast (i.e. fasted), or with a 4 h period of re-feeding following t he overnight fast (i.e. refed). A pattern of fasting-induced expression of *Agpat4* was evident in heart, kidney, and renal white adipose, with partial or complete suppression of *Agpat4* induction occurring upon the reintroduction of nutrients (Figs. 16*B*, *C*, *D*). The level of induction was sizable. Hearts from fasted mice showed an approximate 12.5-fold increase in *Agpat4* expression, kidneys showed an ~18.5-fold increase, and white-adipose showed an ~4-fold increase in expression when compared to *Agpat4* levels in the non-fasted state. Upon re-feeding, kidney *Agpat4* expression returned to non-fasted levels most rapidly, and was the only organ to exhibit a complete suppression of fasting-induced Agpat4 by 4 h following the reintroduction of food. Despite the similarity in *Apgat4* regulation between heart, kidney, and WAT, organ-specific differences were apparent. In particular, brain *Agpat4*

expression was not significantly up- or down-regulated during the various metabolic states (Fig. 16*A*). And, opposite to the pattern of regulation observed in heart, kidney, and WAT, livers from fasted mice showed a 6-fold down-regulation of *Agpat4* as compared to the non-fasted state, which was followed by an approximate 12-fold induction of *Agpat4* 4 h after re-feeding (Fig. 16*E*). These data indicate a complex pattern of Agpat4 regulation in response to changing developmental and metabolic conditions.

Chapter Six – Discussion

In the current study, I report the characterization of acyl-CoA-dependent lysophosphatidic acid acyltransferase 4 (LPAAT4/AGPAT4) that functions in PA remodeling. To the best of our knowledge, this is the first study that identifies AGPAT4 localization to the mitochondria and function in PI synthesis.

In agreement with the observations of others (19,25,33), we found that AGPAT4 is abundantly expressed in murine whole brain tissue. We extended these findings by investigating the expression of AGPAT4 in various subregions of the central nervous system including the olfactory bulbs, hippocampus, cerebellum, cortex, and brain stem, and found similar expression throughout. Furthermore, we detected AGPAT4 in both cultured primary cortical neurons and glial cells, indicating an important role for this enzyme throughout neural tissue. Examination of multiple other organs indicated largely ubiquitous expression of *Agpat4*, albeit at varying levels, in tissues as diverse as liver, kidney, lung, heart, renal white adipose tissue, and skeletal muscle. Although all studies to date (19,25,33) have reported the highest level of *Agpat4* expression in brain, they also typically show *Agpat4* expression in most tissues, albeit with some variation between reports, including ours. For example, while we, and others (25) found abundant *Agpat4* in adipose tissue, additional reports indicated detection of adipose *Agpat4* mRNA at <10% of that found in brain (33). Similarly, while we found relatively abundant *Agpat4* expression in heart, others report that this mRNA is barely detected in that organ (19,25,33). Abundance of *Agpat4* mRNA in lung also ranges from barely detectable (21), to present at ~50% of the abundance in brain, or higher (19,25,33).

Subcellular analysis of whole brain homogenates from wild type mice determined that AGPAT4 localizes predominately to the mitochondria, and also shows a small fraction in the

nuclear envelope. Although AGPAT5 has also been shown to localize to the mitochondria, the sub-mitochondrial fraction where this enzyme is resident has not yet been determined (11). A similar pattern of subcellular localization was evident for overexpressed AGPAT4. Our findings differ from one previous report. In that work, researchers found AGPAT4 localization to be highest in the ER, although subcellular fractionation was not employed (33). To the best of our knowledge, our findings make AGPAT4 only the second known AGPAT/LPAAT to preferentially localize to the mitochondria. Prior to this work, only AGPAT5 has been shown to have predominant mitochondrial localization (25), with most other AGPAT isoforms localizing preferentially to the endoplasmic reticulum (11).

This initial discovery signified a likely role for AGPAT4 in mitochondrial lipid metabolism. Although the major cellular phospholipid species PC, PE, PS, PG, PI, PA, and CL can be detected in essentially all cellular organellar membranes to some extent, mitochondria show a highly characteristic pattern of PL species that is relatively well-conserved across mammals, yeast, and plants (39). The major species in the mammalian mitochondrial phospholipid bilayers are reported to be PC and PE, together forming over 2/3 of total phospholipid, and CL (15-20%) (3,39,40) and PI (~10%), with PS, PG, and PA together compromising only ~3% (39). In contrast, the phospholipid bilayers of mammalian plasma membranes have a much different composition, where the major species are PC (34%), PE (33%), and PS (10.5%), with PI and CL compromising only ~5% in total (41). The localization of AGPAT4 to the mitochondrial membrane suggested that this enzyme may have activity with other lysophospholipid species, including those that are enriched in this organelle. Analysis of the biochemical function of AGPAT4, however, demonstrated that the predominant *in vitro* enzymatic activity is the acyl-CoA-dependent synthesis of PA from LPA, precluding a direct

role for this enzyme in the synthesis of mitochondrial PG, CL, PI, PC, PE, or PS. AGPAT4 showed a clear preference for activity at pH 7.4. This is in agreement with the finding of a predominate mitochondrial localization and it further suggests that AGPAT4 may function on the outer surface of the mitochondrion, where the cytoplasmic pH is ~7.4, rather than in the matrix where the pH is closer to 7.8.

The role of AGPAT4 in PL synthesis *in vivo* was also investigated. PA is an important branching point in the Kennedy pathway. As end products, it can produce TAG, or feed into a wide variety of pathways to produce PLs including mitochondria-associated species. We focused our investigation on PL products of PA metabolism, rather than TAG, since the brain has extremely limited quantities of stored neutral lipid (42). To determine effects of increased PA synthesis on cellular phospholipid species, Sf9 cells overexpressing AGPAT4 were extracted and resolved to separate phospholipid from neutral lipid. Isolated PL were further resolved by TLC, scraped, and quantified by determination of associated fatty acids using GC. Surprisingly, however, only one major PL species was elevated – PI. A specific and highly statistically significant increase in PI content of Sf9 cells was observed with overexpression of AGPAT4. This effect could not be attributed to a non-specific change, such as an increase in mitochondrial content, since other mitochondria-specific PL species such as CL and PG were not elevated.

The finding of a decrease in PI is of particular interest, considering that AGPAT4 is most highly expressed in the brain. PI is a relatively minor phospholipid in most tissues (41,43), but is enriched in the brain, particularly during aging (44). PI has many functions in different tissues, since it acts as a source for polyphosphorylated phosphoinositides that are released from membrane-bound PI by the action of phospholipase C to act in myriad signaling pathways. In brain, these signaling events include regulation of neurotransmission (45), and neuronal

exocytosis (46), with phosphoinositides implicated in regulating functional and structural plasticity (47-49). Loss of *Agpat4* in the present study caused a greater than 50% reduction in brain levels of PI. This effect is substantial, far exceeding the slight (<10%) reduction observed in mice that have a deletion of *Lpiat1*, the enzyme that governs PI remodeling by acylating LPI (50). Agpat4 is therefore likely to play a role in the regulation of brain phosphoinositide-mediated signaling and function.

Overexpression of AGPAT4 in Sf9 cells resulted in the enrichment of endogenous cellular PA with total saturated fatty acids. In particular, significant increases in lauric (C12:0) and arachidic (C20:0) acid were evident. Interestingly, the content of docosahexanoic acid in PA was not enriched by overexpression of AGPAT4 in Sf9 cells, which is in contrast to a previous report by Eto et al, who found that AGPAT4 preferentially esterifies DHA at the sn-2 position of LPA. (33).

To provide preliminary investigation of a physiological function, we examined the regulation of *Agpat4* gene expression with changing nutritional conditions, and during embryonic development. We found significant variation in the levels of *Agpat4* in many tissues between the non-fasted, fasted, and refed states. Interestingly, this variation was not consistent among tissues, but rather showed a distinct pattern whereby hepatic *Agpat4* mRNA expression was suppressed by fasting, but *Agpat4* in extra-hepatic tissues, except for brain, was induced by fasting then partially or completely repressed to non-fasted levels by subsequent refeeding. Brain *Agpat4* expression, uniquely, was refractive to changes in metabolic state. The reason for this differential expression is currently unknown, but the inverse regulation of this enzyme in different tissues, and lack of metabolic regulation in brain, suggest that complex transcriptional mechanisms are likely at work beyond the action of a single, major regulatory influence such as

insulin signaling. Of interest, our finding of significant tissue-specific differences in expression of *Agpat4* with changing metabolic conditions may help to explain the variability in this measure between individual studies, since nutritional state was not standardized either across or within studies (19,25,33). In future, researchers should take care to control for this variable in experiments on gene expression.

Elucidation of the factors governing transcriptional regulation of Agpat4 will also be important for understanding the role of this enzyme in embryonic development. *Agpat4* expression almost quadrupled between developmental days 10.5 and 14.5, and then fell to 15% of developmental day 10.5 levels immediately prior to birth. The reason for this change is currently unknown, and further studies will be required to determine whether this reflects specific changes occurring during these developmental timeframes, such as expansion of neural tissue, or widespread cellular expression during rapid organogenesis and development.

Understanding cellular PI synthesis has important consequences for health and disease. Changes in mitochondrial phospholipid composition have been shown to alter mitochondrial respiration (51), and can induce cell apoptosis (52). Clinically, changes in mitochondrial phospholipid synthesis and membrane composition have been shown to cause disease, with changes in phosphoinositides playing a role in Lowe Syndrome (53), Dent disease (54), cancers (55-59), diabetes (60,61), and neurological defects such as Alzheimer's disease and Down Syndrome (62-64). Future studies will focus on determining the role of altered AGPAT4-mediated PI synthesis in mitochondrial metabolism and brain function.

Chapter Seven – Study Limitations and Future Directions

Limitations

The major shortcoming in our identification and characterization of AGPAT4 is the use of baculoviral overexpression of this enzyme in the *in vitro* and *in vivo* characterization. There is no direct evidence that endogenous AGPAT4 functions in a similar manner to overexpressed enzyme. Immortal cell lines that show a high endogenous expression of AGPAT4 can be used to investigate the silencing of this gene by small interfering RNAs (siRNAs) to determine whether the loss of native AGPAT4 decreases PA remodeling and *de novo* PA synthesis. Gene ablation of *Agpat4* in mice is another approach to investigate this question. Another limitation to this work is that crude protein lysates were used in characterizing this enzyme, and therefore may have contained other membrane-bound and non-membrane-bound proteins that could affect the assay, either indirectly by modifying activity of AGPAT4, or directly by functioning to produce additional AGPAT activity or affect PA synthesis or breakdown. The difficulty in purifying AGPAT for *in vitro assay* is a challenge faced by most acyltransferase researchers, given that the majority of these enzymes are integral membrane proteins. AGPAT4 is predicted to have 3-5 transmembrane domains (Fig. 3), which renders it very difficult to remove from the membrane. Since our studies include recombinant AGPAT4 with 6x His tags, purifying this protein with a Ni-NTA purification system may yield purer protein that can be used in enzymological experiments, although the amount of protein generated may be severely limited. Future work will address these limitations, and extend studies reported in this thesis.

Future Directions

Phospholipids such as phosphatidylinositol are critical in cell signaling pathways needed to maintain a healthy state (46). In disease states, mitochondria can be oxidized by reactive oxygen species and undergo mitophagy, or mitochondrial-mediated apoptosis. Several mitochondrial-associated phospholipids including cardiolipin and phosphatidylinositol are potent regulators of these cellular processes (65-76). Mitochondrial-mediated apoptosis is a form of programmed cell death occurring due to factors released by damaged or dysfunctional mitochondria (75). It has been shown that phosphatidylinositol 3-phosphate is a key factor in mediating this process (65). Future work will be required to first confirm that AGPAT4 regulates PI synthesis *in vivo*, and then to determine the role of AGPAT4-mediated regulation of PI synthesis in brain mitochondrial functions including apoptosis, mitosis, and cellular energy metabolism. Species profiling of PI generated by AGPAT4 will be of particular interest, since PI in mammalian brain is generally esterified with stearic acid at the sn-1 position, and arachidonic acid at the sn-2 position (54-57), suggesting that the type and level of unsaturated fatty acids in PI may be important for cellular and mitochondrial functioning of this PL. Whether variation in the fatty acyl specificity of AGPAT4-derived PI occurs, and whether this alters the function of PI in cells, will be the focus of subsequent research.

References

1. Athenstaedt, K., and Daum, G. (1999) Phosphatidic acid, a key intermediate in lipid metabolism. *European journal of biochemistry / FEBS* **266**, 1-16
2. Kooijman, E. E., and Burger, K. N. (2009) Biophysics and function of phosphatidic acid: a molecular perspective. *Biochimica et biophysica acta* **1791**, 881-888
3. de Kroon, A. I., Dolis, D., Mayer, A., Lill, R., and de Kruijff, B. (1997) Phospholipid composition of highly purified mitochondrial outer membranes of rat liver and Neurospora crassa. Is cardiolipin present in the mitochondrial outer membrane? *Biochimica et biophysica acta* **1325**, 108-116
4. Hsia, J. C., Chen, W. L., Long, R. A., Wong, L. T., and Kalow, W. (1972) Existence of phospholipid bilayer structure in the inner membrane of mitochondria. *Proceedings of the National Academy of Sciences of the United States of America* **69**, 3412-3415
5. Kennedy, E. P., and Weiss, S. B. (1956) The function of cytidine coenzymes in the biosynthesis of phospholipides. *The Journal of biological chemistry* **222**, 193-214
6. Lands, W. E. (1958) Metabolism of glycerolipides; a comparison of lecithin and triglyceride synthesis. *The Journal of biological chemistry* **231**, 883-888
7. Yet, S. F., Lee, S., Hahm, Y. T., and Sul, H. S. (1993) Expression and identification of p90 as the murine mitochondrial glycerol-3-phosphate acyltransferase. *Biochemistry* **32**, 9486-9491
8. Lewin, T. M., Schwerbrock, N. M., Lee, D. P., and Coleman, R. A. (2004) Identification of a new glycerol-3-phosphate acyltransferase isoenzyme, mtGPAT2, in mitochondria. *The Journal of biological chemistry* **279**, 13488-13495
9. Nagle, C. A., Vergnes, L., Dejong, H., Wang, S., Lewin, T. M., Reue, K., and Coleman, R. A. (2008) Identification of a novel sn-glycerol-3-phosphate acyltransferase isoform, GPAT4, as the enzyme deficient in Agpat6-/- mice. *Journal of lipid research* **49**, 823-831
10. Cao, J., Li, J. L., Li, D., Tobin, J. F., and Gimeno, R. E. (2006) Molecular identification of microsomal acyl-CoA:glycerol-3-phosphate acyltransferase, a key enzyme in de novo triacylglycerol synthesis. *Proceedings of the National Academy of Sciences of the United States of America* **103**, 19695-19700
11. Kitson, A. P., Stark, K. D., and Duncan, R. E. (2012) Enzymes in brain phospholipid docosahexaenoic acid accretion: a PL-ethora of potential PL-ayers. *Prostaglandins, leukotrienes, and essential fatty acids* **87**, 1-10
12. Chakraborty, T. R., Vancura, A., Balija, V. S., and Haldar, D. (1999) Phosphatidic acid synthesis in mitochondria. Topography of formation and transmembrane migration. *The Journal of biological chemistry* **274**, 29786-29790
13. Hatch, G. M. (2004) Cell biology of cardiac mitochondrial phospholipids. *Biochemistry and cell biology = Biochimie et biologie cellulaire* **82**, 99-112
14. Bayburt, T., Yu, B. Z., Lin, H. K., Browning, J., Jain, M. K., and Gelb, M. H. (1993) Human nonpancreatic secreted phospholipase A2: interfacial parameters, substrate specificities, and competitive inhibitors. *Biochemistry* **32**, 573-582
15. Burke, J. E., and Dennis, E. A. (2009) Phospholipase A2 structure/function, mechanism, and signaling. *Journal of lipid research* **50 Suppl**, S237-242
16. Diez, E., Louis-Flamberg, P., Hall, R. H., and Mayer, R. J. (1992) Substrate specificities and properties of human phospholipases A2 in a mixed vesicle model. *The Journal of biological chemistry* **267**, 18342-18348

17. Gesquiere, L., Cho, W., and Subbaiah, P. V. (2002) Role of group IIa and group V secretory phospholipases A(2) in the metabolism of lipoproteins. Substrate specificities of the enzymes and the regulation of their activities by sphingomyelin. *Biochemistry* **41**, 4911-4920
18. Cao, J., Shan, D., Revett, T., Li, D., Wu, L., Liu, W., Tobin, J. F., and Gimeno, R. E. (2008) Molecular identification of a novel mammalian brain isoform of acyl-CoA:lysophospholipid acyltransferase with prominent ethanolamine lysophospholipid acylating activity, LPEAT2. *The Journal of biological chemistry* **283**, 19049-19057
19. Lu, B., Jiang, Y. J., Zhou, Y., Xu, F. Y., Hatch, G. M., and Choy, P. C. (2005) Cloning and characterization of murine 1-acyl-sn-glycerol 3-phosphate acyltransferases and their regulation by PPARalpha in murine heart. *The Biochemical journal* **385**, 469-477
20. Chen, Y. Q., Kuo, M. S., Li, S., Bui, H. H., Peake, D. A., Sanders, P. E., Thibodeaux, S. J., Chu, S., Qian, Y. W., Zhao, Y., Bredt, D. S., Moller, D. E., Konrad, R. J., Beigneux, A. P., Young, S. G., and Cao, G. (2008) AGPAT6 is a novel microsomal glycerol-3-phosphate acyltransferase. *The Journal of biological chemistry* **283**, 10048-10057
21. Ye, G. M., Chen, C., Huang, S., Han, D. D., Guo, J. H., Wan, B., and Yu, L. (2005) Cloning and characterization a novel human 1-acyl-sn-glycerol-3-phosphate acyltransferase gene AGPAT7. *DNA sequence : the journal of DNA sequencing and mapping* **16**, 386-390
22. Agarwal, A. K., Barnes, R. I., and Garg, A. (2006) Functional characterization of human 1-acylglycerol-3-phosphate acyltransferase isoform 8: cloning, tissue distribution, gene structure, and enzymatic activity. *Archives of biochemistry and biophysics* **449**, 64-76
23. Agarwal, A. K., and Garg, A. (2010) Enzymatic activity of the human 1-acylglycerol-3-phosphate-O-acyltransferase isoform 11: upregulated in breast and cervical cancers. *Journal of lipid research* **51**, 2143-2152
24. Agarwal, A. K., Sukumaran, S., Bartz, R., Barnes, R. I., and Garg, A. (2007) Functional characterization of human 1-acylglycerol-3-phosphate-O-acyltransferase isoform 9: cloning, tissue distribution, gene structure, and enzymatic activity. *The Journal of endocrinology* **193**, 445-457
25. Prasad, S. S., Garg, A., and Agarwal, A. K. (2011) Enzymatic activities of the human AGPAT isoform 3 and isoform 5: localization of AGPAT5 to mitochondria. *Journal of lipid research* **52**, 451-462
26. Sukumaran, S., Barnes, R. I., Garg, A., and Agarwal, A. K. (2009) Functional characterization of the human 1-acylglycerol-3-phosphate-O-acyltransferase isoform 10/glycerol-3-phosphate acyltransferase isoform 3. *Journal of molecular endocrinology* **42**, 469-478
27. Cao, J., Liu, Y., Lockwood, J., Burn, P., and Shi, Y. (2004) A novel cardiolipin-remodeling pathway revealed by a gene encoding an endoplasmic reticulum-associated acyl-CoA:lysocardiolipin acyltransferase (ALCAT1) in mouse. *The Journal of biological chemistry* **279**, 31727-31734
28. Kume, K., and Shimizu, T. (1997) cDNA cloning and expression of murine 1-acyl-sn-glycerol-3-phosphate acyltransferase. *Biochemical and biophysical research communications* **237**, 663-666
29. Agarwal, A. K., Sukumaran, S., Cortes, V. A., Tunison, K., Mizrachi, D., Sankella, S., Gerard, R. D., Horton, J. D., and Garg, A. (2011) Human 1-acylglycerol-3-phosphate O-acyltransferase isoforms 1 and 2: biochemical characterization and inability to rescue

hepatic steatosis in Agpat2(-/-) gene lipodystrophic mice. *The Journal of biological chemistry* **286**, 37676-37691
30. Aguado, B., and Campbell, R. D. (1998) Characterization of a human lysophosphatidic acid acyltransferase that is encoded by a gene located in the class III region of the human major histocompatibility complex. *The Journal of biological chemistry* **273**, 4096-4105
31. Yuki, K., Shindou, H., Hishikawa, D., and Shimizu, T. (2009) Characterization of mouse lysophosphatidic acid acyltransferase 3: an enzyme with dual functions in the testis. *Journal of lipid research* **50**, 860-869
32. Lewin, T. M., Wang, P., and Coleman, R. A. (1999) Analysis of amino acid motifs diagnostic for the sn-glycerol-3-phosphate acyltransferase reaction. *Biochemistry* **38**, 5764-5771
33. Eto, M., Shindou, H., and Shimizu, T. (2014) A novel lysophosphatidic acid acyltransferase enzyme (LPAAT4) with a possible role for incorporating docosahexaenoic acid into brain glycerophospholipids. *Biochemical and biophysical research communications* **443**, 718-724
34. Beigneux, A. P., Vergnes, L., Qiao, X., Quatela, S., Davis, R., Watkins, S. M., Coleman, R. A., Walzem, R. L., Philips, M., Reue, K., and Young, S. G. (2006) Agpat6--a novel lipid biosynthetic gene required for triacylglycerol production in mammary epithelium. *Journal of lipid research* **47**, 734-744
35. Bligh, E. G., and Dyer, W. J. (1959) A rapid method of total lipid extraction and purification. *Canadian journal of biochemistry and physiology* **37**, 911-917
36. Folch, J., Lees, M., and Sloane Stanley, G. H. (1957) A simple method for the isolation and purification of total lipides from animal tissues. *The Journal of biological chemistry* **226**, 497-509
37. Metherel, A. H., Taha, A. Y., Izadi, H., and Stark, K. D. (2009) The application of ultrasound energy to increase lipid extraction throughput of solid matrix samples (flaxseed). *Prostaglandins, leukotrienes, and essential fatty acids* **81**, 417-423
38. Dimauro, I., Pearson, T., Caporossi, D., and Jackson, M. J. (2012) A simple protocol for the subcellular fractionation of skeletal muscle cells and tissue. *BMC research notes* **5**, 513
39. Mejia, E. M., and Hatch, G. M. (2015) Mitochondrial phospholipids: role in mitochondrial function. *Journal of bioenergetics and biomembranes*
40. Daum, G., and Vance, J. E. (1997) Import of lipids into mitochondria. *Progress in lipid research* **36**, 103-130
41. Diagne, A., Fauvel, J., Record, M., Chap, H., and Douste-Blazy, L. (1984) Studies on ether phospholipids. II. Comparative composition of various tissues from human, rat and guinea pig. *Biochimica et biophysica acta* **793**, 221-231
42. Owen, O. E., Morgan, A. P., Kemp, H. G., Sullivan, J. M., Herrera, M. G., and Cahill, G. F., Jr. (1967) Brain metabolism during fasting. *The Journal of clinical investigation* **46**, 1589-1595
43. Daum, G. (1985) Lipids of mitochondria. *Biochimica et biophysica acta* **822**, 1-42
44. Modi, H. R., Katyare, S. S., and Patel, M. A. (2008) Ageing-induced alterations in lipid/phospholipid profiles of rat brain and liver mitochondria: implications for mitochondrial energy-linked functions. *The Journal of membrane biology* **221**, 51-60
45. Zhang, Y., McCartney, A. J., Zolov, S. N., Ferguson, C. J., Meisler, M. H., Sutton, M. A., and Weisman, L. S. (2012) Modulation of synaptic function by VAC14, a protein that

regulates the phosphoinositides PI(3,5)P(2) and PI(5)P. *The EMBO journal* **31**, 3442-3456
46. Vicinanza, M., D'Angelo, G., Di Campli, A., and De Matteis, M. A. (2008) *Function and dysfunction of the PI system in membrane trafficking*,
47. Ueno, T., Falkenburger, B. H., Pohlmeyer, C., and Inoue, T. (2011) Triggering actin comets versus membrane ruffles: distinctive effects of phosphoinositides on actin reorganization. *Science signaling* **4**, ra87
48. Sanna, P. P., Cammalleri, M., Berton, F., Simpson, C., Lutjens, R., Bloom, F. E., and Francesconi, W. (2002) Phosphatidylinositol 3-kinase is required for the expression but not for the induction or the maintenance of long-term potentiation in the hippocampal CA1 region. *The Journal of neuroscience : the official journal of the Society for Neuroscience* **22**, 3359-3365
49. Arendt, K. L., Royo, M., Fernandez-Monreal, M., Knafo, S., Petrok, C. N., Martens, J. R., and Esteban, J. A. (2010) PIP3 controls synaptic function by maintaining AMPA receptor clustering at the postsynaptic membrane. *Nature neuroscience* **13**, 36-44
50. Lee, H. C., Inoue, T., Sasaki, J., Kubo, T., Matsuda, S., Nakasaki, Y., Hattori, M., Tanaka, F., Udagawa, O., Kono, N., Itoh, T., Ogiso, H., Taguchi, R., Arita, M., Sasaki, T., and Arai, H. (2012) LPIAT1 regulates arachidonic acid content in phosphatidylinositol and is required for cortical lamination in mice. *Molecular biology of the cell* **23**, 4689-4700
51. Ohtsuka, T., Nishijima, M., and Akamatsu, Y. (1993) A somatic cell mutant defective in phosphatidylglycerophosphate synthase, with impaired phosphatidylglycerol and cardiolipin biosynthesis. *The Journal of biological chemistry* **268**, 22908-22913
52. Fadok, V. A., and Henson, P. M. (2003) Apoptosis: giving phosphatidylserine recognition an assist--with a twist. *Current biology : CB* **13**, R655-657
53. Attree, O., Olivos, I. M., Okabe, I., Bailey, L. C., Nelson, D. L., Lewis, R. A., McInnes, R. R., and Nussbaum, R. L. (1992) The Lowe's oculocerebrorenal syndrome gene encodes a protein highly homologous to inositol polyphosphate-5-phosphatase. *Nature* **358**, 239-242
54. Hoopes, R. R., Jr., Shrimpton, A. E., Knohl, S. J., Hueber, P., Hoppe, B., Matyus, J., Simckes, A., Tasic, V., Toenshoff, B., Suchy, S. F., Nussbaum, R. L., and Scheinman, S. J. (2005) Dent Disease with mutations in OCRL1. *American journal of human genetics* **76**, 260-267
55. Carracedo, A., and Pandolfi, P. P. (2008) The PTEN-PI3K pathway: of feedbacks and cross-talks. *Oncogene* **27**, 5527-5541
56. Luo, J., Manning, B. D., and Cantley, L. C. (2003) Targeting the PI3K-Akt pathway in human cancer: rationale and promise. *Cancer cell* **4**, 257-262
57. Osaki, M., Oshimura, M., and Ito, H. (2004) PI3K-Akt pathway: its functions and alterations in human cancer. *Apoptosis : an international journal on programmed cell death* **9**, 667-676
58. Salmena, L., Carracedo, A., and Pandolfi, P. P. (2008) Tenets of PTEN tumor suppression. *Cell* **133**, 403-414
59. Yuan, T. L., and Cantley, L. C. (2008) PI3K pathway alterations in cancer: variations on a theme. *Oncogene* **27**, 5497-5510
60. Marion, E., Kaisaki, P. J., Pouillon, V., Gueydan, C., Levy, J. C., Bodson, A., Krzentowski, G., Daubresse, J. C., Mockel, J., Behrends, J., Servais, G., Szpirer, C.,

Kruys, V., Gauguier, D., and Schurmans, S. (2002) The gene INPPL1, encoding the lipid phosphatase SHIP2, is a candidate for type 2 diabetes in rat and man. *Diabetes* **51**, 2012-2017

61. Wada, T., Sasaoka, T., Funaki, M., Hori, H., Murakami, S., Ishiki, M., Haruta, T., Asano, T., Ogawa, W., Ishihara, H., and Kobayashi, M. (2001) Overexpression of SH2-containing inositol phosphatase 2 results in negative regulation of insulin-induced metabolic actions in 3T3-L1 adipocytes via its 5'-phosphatase catalytic activity. *Molecular and cellular biology* **21**, 1633-1646
62. Cremona, O., Di Paolo, G., Wenk, M. R., Luthi, A., Kim, W. T., Takei, K., Daniell, L., Nemoto, Y., Shears, S. B., Flavell, R. A., McCormick, D. A., and De Camilli, P. (1999) Essential role of phosphoinositide metabolism in synaptic vesicle recycling. *Cell* **99**, 179-188
63. Di Paolo, G., and De Camilli, P. (2006) Phosphoinositides in cell regulation and membrane dynamics. *Nature* **443**, 651-657
64. Gong, L. W., and De Camilli, P. (2008) Regulation of postsynaptic AMPA responses by synaptojanin 1. *Proceedings of the National Academy of Sciences of the United States of America* **105**, 17561-17566
65. Burman, C., and Ktistakis, N. T. (2010) Regulation of autophagy by phosphatidylinositol 3-phosphate. *FEBS letters* **584**, 1302-1312
66. Chu, C. T., Ji, J., Dagda, R. K., Jiang, J. F., Tyurina, Y. Y., Kapralov, A. A., Tyurin, V. A., Yanamala, N., Shrivastava, I. H., Mohammadyani, D., Qiang Wang, K. Z., Zhu, J., Klein-Seetharaman, J., Balasubramanian, K., Amoscato, A. A., Borisenko, G., Huang, Z., Gusdon, A. M., Cheikhi, A., Steer, E. K., Wang, R., Baty, C., Watkins, S., Bahar, I., Bayir, H., and Kagan, V. E. (2013) Cardiolipin externalization to the outer mitochondrial membrane acts as an elimination signal for mitophagy in neuronal cells. *Nature cell biology* **15**, 1197-1205
67. Ashrafi, G., and Schwarz, T. L. (2013) The pathways of mitophagy for quality control and clearance of mitochondria. *Cell death and differentiation* **20**, 31-42
68. Glick, D., Barth, S., and Macleod, K. F. (2010) Autophagy: cellular and molecular mechanisms. *The Journal of pathology* **221**, 3-12
69. Cheng, H., Mancuso, D. J., Jiang, X., Guan, S., Yang, J., Yang, K., Sun, G., Gross, R. W., and Han, X. (2008) Shotgun lipidomics reveals the temporally dependent, highly diversified cardiolipin profile in the mammalian brain: temporally coordinated postnatal diversification of cardiolipin molecular species with neuronal remodeling. *Biochemistry* **47**, 5869-5880
70. Claypool, S. M., Oktay, Y., Boontheung, P., Loo, J. A., and Koehler, C. M. (2008) Cardiolipin defines the interactome of the major ADP/ATP carrier protein of the mitochondrial inner membrane. *The Journal of cell biology* **182**, 937-950
71. Garcia Fernandez, M., Troiano, L., Moretti, L., Nasi, M., Pinti, M., Salvioli, S., Dobrucki, J., and Cossarizza, A. (2002) Early changes in intramitochondrial cardiolipin distribution during apoptosis. *Cell growth & differentiation : the molecular biology journal of the American Association for Cancer Research* **13**, 449-455
72. Raemy, E., and Martinou, J. C. (2014) Involvement of cardiolipin in tBID-induced activation of BAX during apoptosis. *Chemistry and physics of lipids* **179**, 70-74
73. Schug, Z. T., and Gottlieb, E. (2009) Cardiolipin acts as a mitochondrial signalling platform to launch apoptosis. *Biochimica et biophysica acta* **1788**, 2022-2031

74. Sorice, M., Circella, A., Cristea, I. M., Garofalo, T., Di Renzo, L., Alessandri, C., Valesini, G., and Esposti, M. D. (2004) Cardiolipin and its metabolites move from mitochondria to other cellular membranes during death receptor-mediated apoptosis. *Cell death and differentiation* **11**, 1133-1145
75. Wang, C., and Youle, R. J. (2009) The role of mitochondria in apoptosis*. *Annual review of genetics* **43**, 95-118
76. Kim, I., and Lemasters, J. J. (2011) Mitophagy selectively degrades individual damaged mitochondria after photoirradiation. *Antioxidants & redox signaling* **14**, 1919-1928

Appendix

Table 3: Fatty acyl species in PA from Sf9 cells overexpressing AGPAT4 or control vector.

Fatty Acyl Species	μmol fatty acid ± S.E.M. / mg protein		P-value
	Control	AGPAT4	
10:0	0.01 ± 0.01	0.00 ± 0.00	0.55
12:0	0.07 ± 0.03	0.19 ± 0.01	0.0017
14:0	0.55 ± 0.24	0.61 ± 0.14	0.69
16:0	5.22 ± 2.17	9.20 ± 2.14	0.18
18:0	7.32 ± 2.66	13.14 ± 3.54	0.18
20:0	0.93 ± 0.25	4.53 ± 1.32	0.02
22:0	0.69 ± 0.25	1.48 ± 0.39	0.10
24:0	0.19 ± 0.07	0.36 ± 0.15	0.28
Σ SFA	15.00 ± 5.14	29.55 ± 6.89	0.09
12:1	0.01 ± 0.01	0.02 ± 0.01	0.25
14:1	0.01 ± 0.01	0.02 ± 0.00	0.60
16:1	0.84 ± 0.18	1.17 ± 0.27	0.29
18:1n-7	0.25 ± 0.06	0.22 ± 0.04	0.77
18:1n-9	1.33 ± 0.22	1.74 ± 0.32	0.27
20:1n-9	0.03 ± 0.01	0.04 ± 0.01	0.62
22:1n-9	0.35 ± 0.15	0.53 ± 0.20	0.44
24:1n-9	0.05 ± 0.02	0.06 ± 0.03	0.72
Σ MUFA	2.87 ± 0.50	3.79 ± 0.55	0.20
18:2n-6	0.15 ± 0.03	0.17 ± 0.07	0.73
18:3n-6	0.00 ± 0.00	0.01 ± 0.01	0.25
20:2n-6	0.01 ± 0.00	0.03 ± 0.02	0.25
20:3n-6	0.03 ± 0.03	0.04 ± 0.02	0.87
20:4n-6	0.04 ± 0.03	0.04 ± 0.02	0.92
22:2n-6	0.10 ± 0.05	0.13 ± 0.05	0.77
22:4n-6	0.14 ± 0.05	0.22 ± 0.10	0.44
22:5n-6	0.11 ± 0.06	0.11 ± 0.03	0.93
Σ n-6 PUFA	0.59 ± 0.24	0.74 ± 0.29	0.65
18:3n-3	0.01 ± 0.00	0.01 ± 0.01	0.60
20:3n-3	0.32 ± 0.13	0.49 ± 0.19	0.46
20:5n-3	0.03 ± 0.02	0.05 ± 0.02	0.43
22:5n-3	0.02 ± 0.01	0.02 ± 0.01	0.96
22:6n-3	0.03 ± 0.02	0.06 ± 0.02	0.17
Σ n-3 PUFA	0.41 ± 0.18	0.64 ± 0.24	0.41